Thermal Cycling of Out-Of-Autoclave Thermosetting Composite Materials

Soheila Mahdavi

A thesis

in

The Department

of

Mechanical and Industrial Engineering

Presented in Partial Fulfillment of the Requirements

for the Degree of

Master of Applied Science (Mechanical Engineering)

at Concordia University

Montreal, Quebec, Canada

March 2017

CONCORDIA UNIVERSITY

School of Graduate Studies

This is to certify that the thesis prepared

By: **Soheila Mahdavi**

Entitled: **Thermal Cycling of Out-Of-Autoclave Thermosetting Composite Materials**

and submitted in partial fulfillment of the requirements for the degree of

Master of Applied Sciences (Mechanical Engineering) at Concordia University

complies with the regulations of the University and meets the accepted standards with respect to originality and quality.

Signed by the final Examining Committee:

Dr. Chevy Chen _____ Chair

Dr. Robin Drew _____ Examiner

Dr. Saifur Rahaman _____ Examiner

Dr. Mehdi Hojjati _____ Supervisor

Approved by: _____

Chair of Department or Graduate Program Director

_____

Dean, Faculty of Engineering and Computer Science

Date: March 2, 2017

Abstract

Thermal Cycling of Out-Of-Autoclave Thermosetting Composite Materials

Soheila Mahdavi

Carbon fiber reinforced polymer composites have been widely used in space industries for manufacturing of spacecraft structures, satellite-panels and antennas. Composite materials in space undergo harsh environmental conditions. One of the most environmental effects during the life of a satellite antenna is thermal cycling during which the composite endures a large temperature difference between −196°C and +180°C, depending on operational condition. On the other hand, composite structures for space applications are often cured in an autoclave to achieve the required space grade quality which is limited and expensive. Therefore, fabrication of large structures using out-of-autoclave (OOA) with the same performance as autoclave with lower costs is of interest of many industries. Composite parts cured inside an oven have higher void content than the ones cured in the autoclave. This thesis aims to study the effect of thermal cycling on the mechanical and thermal properties of flat laminates made of unidirectional (UD) and woven fabric OOA materials as well as a sandwich panel. A toughened epoxy prepreg reinforced by carbon fibers was used to manufacture flat laminates by the hand layup and cured inside the oven. Coupon samples were cut and subjected to different number of thermal cycles (30, 60, 100, 150, 200, 350) by dipping into the liquid nitrogen (−196°C) and then transferring to the oven (+140°C). Afterwards, different material properties were measured including: interlaminar shear strength (ILSS) in three-point bending, viscoelastic properties (loss and storage modulus and tan δ) and glass transition temperature (T_g) in DMA, and coefficient of thermal expansion (CTE) in TMA. Besides, optical microscope was utilized to identify damages within the resin. It was identified that the thermal cycling can affect the examined properties by two competing factors: (i) excessive cross-linking in polymer chain due to post-curing at high temperature; (ii) micro-cracks formation due to the induced thermal stresses as a result of matrix/fiber CTE mismatch. It was found that the thermal cycling can cause microcrack formation and propagation around the voids in the laminate and affect its properties.

Keywords

Out-of-autoclave manufacturing, thermal cycling, mechanical properties, thermal properties, microcracks, delamination.

To my husband, Hadi,

for his understanding, patience, and unconditional love;

and to my beloved parents,

for their unending love, encouragement and support.

Even though words have built this thesis that I dedicate to you, they can never express my appreciation enough.

Acknowledgements

I would like to take this opportunity to acknowledge those who have guided, supported, and encouraged me in this work.

First, I wish to express my sincere gratitude to my supervisor, Professor Mehdi Hojjati, whose supervision, assistance, guidance, and support from the initial to the final level enabled me to develop an understanding of the subject. He has supported me with his knowledge and patience whilst allowing me the room to work in my own way. My special thanks goes to Dr. Daniel Rosca and Mr. Heng Wang for their guidance and assistance for all the lab works and test procedures. I also want to thank my colleagues and friends at the Department of Mechanical Engineering and in Concordia Center for Composites (CONCOM), from whom I have learned many things during my time there. Last but not least, I'd like to thank my husband, parents, and the rest of my family. I attribute the level of my Masters degree to their encouragement and effort and without them this thesis, too, would not have been completed or written.

The research work in this thesis was supported by MDA corporation, Stelia North America, the Natural Sciences and Engineering Research Council of Canada (NSERC), and Synergetic Research and Innovation in Aerospace (CRIAQ). I would like to acknowledge their support on this research work. I am also grateful to members of my thesis committee for their valuable time and patience in reviewing this work.

Table of Contents

List of Figures

List of Tables

Chapter 1: Introduction and Scope of Thesis

1.1. Introduction

In the last few decades, fiber-reinforced composite materials have been increasingly used for both structural and non-structural applications. Compared to metallic materials, these composites offer a better combination of strength and modulus, superior strength-to-weight and modulus-to-weight ratios, as well as excellent fatigue strength and fatigue damage tolerance. For these reasons, fiber-reinforced composites have been considered for use as substitutions for metal components in many applications in space, aerospace, military, automotive, sporting goods, marine, etc.[1]. Figure 1-1 shows the composite applications in space and aerospace industry. Particularly for space applications, such as spacecraft and satellite, carbon fiber laminated composites exhibit high stiffness, low coefficient of thermal expansion (CTE), and good dimensional stability in their lifetime, which are very important requirements for space material choice [2].

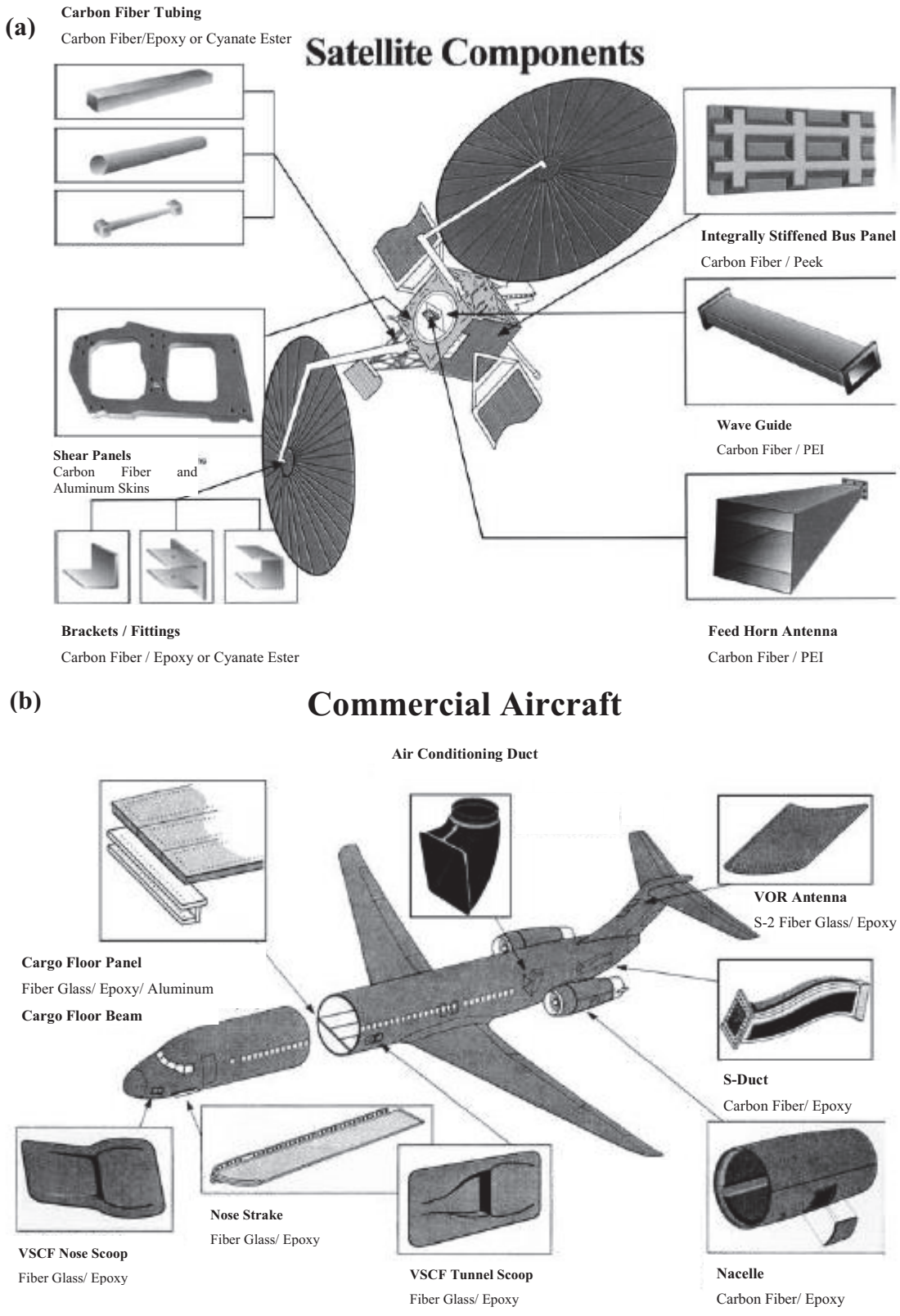

Figure 1-1 Examples of composite applications in (a) satellite, (b) commercial aircraft [3].

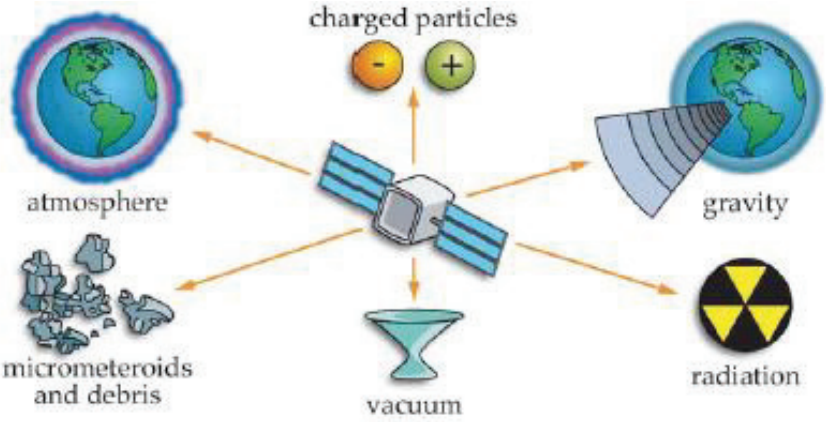

Figure 1-2 A spacecraft exposed to different space environment factors influencing its performance [4].

1.2. Space environmental conditions and its effect on composite materials

Composite materials in space undergo harsh environmental conditions such as ultraviolet (UV) radiation, high vacuum, atomic oxygen (AO), charged particles, man-made debris, micrometeoroids, electromagnetic radiation, and thermal cycles, which all cause material degradation (Figure 1-2) [5].

One of the most important environmental effects during the life of a satellite antenna is thermal cycling in which composite undergoes a large temperature difference ranging from -160˚C to +125˚C [5], [6]. As shown in Figure 1-3, when a satellite travels in its orbit around the earth, it experiences a high temperature difference: once exposed to the sunlight, its temperature increases and when it is in the earth's shadow in umbra (or full shadow) and penumbra (or half shadow) states, its temperature decreases. This recurring temperature variation is known to be thermal cycling. Temperature difference occurs in a relatively short period of time and its intensity depends on the angle of sunlight.

When a composite material is exposed to extreme temperature variation, thermal stresses are induced. Thermal stresses are due to the large difference in the CTE of fiber and matrix. Continuous thermal cycles can cause microcrack formation which leads to fiber–matrix debonding in the composite and finally the material system failure [5], [7]. Figure 1-4 shows the microcracks formed in a carbon polymer composite as a result of cycling between liquid nitrogen temperature and a high temperature of 177 °C.

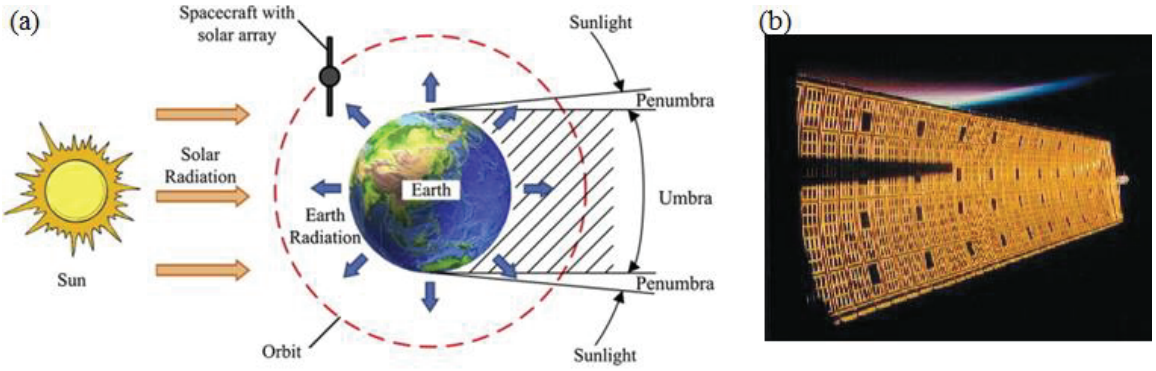

Figure 1-3 A satellite travelling around the earth exposed to sunlight and pathing through umbra and penumbra [8]; (b) a composite solar panel exposed to solar [4].

It is clear that the best practice design of composites exposed to thermal cycles in space requires accurate characterization of their properties. This necessitates development of an experimental procedure which mimics the space situation in order to better evaluate the performance of composite material. Particularly, mechanical and thermal performance of composites exposed to such thermal cycles has drawn a lot of attention from research communities and space industries [9]-[15]. Therefore, the purpose of this research work is to study the mechanical and thermal properties of out-of-autoclave (OOA) carbon fiber epoxy composite after thermal cycling.

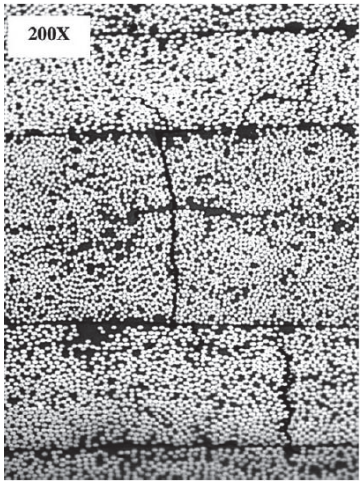

Figure 1-4 Formation of microcrack within a typical carbon polymer composite due to thermal cycling [16].

1.3. Objectives and scopes of thesis

This thesis aims to study the behavior of carbon polymer composite materials exposed to thermal cycling. Main effort is focused on investigating the mechanical and thermal properties of OOA composite laminates due to the thermal cycling. Moreover, microcracking and delamination behavior of sandwich panels considering adhesive effects is also studied. The following points outline the objectives and scopes of the present thesis:

- To study the thermal cycling of OOA thermoset composite materials.
- To have more accurate and practical understanding of the microcrack initiation. A comparison between unidirectional (UD) and woven fabric composite laminates is conducted.
- To study the microcracking effect on the interlaminar shear strength (ILSS), coefficient of thermal expansion (CTE), and dynamic mechanical properties of composites. Thermal cycling effects on these properties of UD and woven fabric materials are compared.
- To describe the interaction between the fiber and matrix at the interface and to examine its effect on the mechanical and thermal behavior of laminates.
- To investigate the microcrack formation due to higher void content in the laminate as a result of OOA manufacturing
- To experimentally study the thermal cycling effect on the microcracking behavior of the composite sandwich panels. Adhesive effect on the state of damage of the plate is considered.

1.4. Chapter summery and outline of thesis

This thesis is written in five different chapters:

Chapter 1 gives a brief description of the space conditions and how composites are affected by these conditions with the focus on thermal cycling. It also provides the hypothesis to reach the thesis objectives.

Chapter 2 provides a literature review on the polymeric matrix composites and reviews the thermal cycling effect on them with focus on mechanical and thermal properties.

Chapter 3 presents the material selected and the manufacturing and preparation methods used for this research. It also covers the different tests utilized to characterize the laminate properties.

Chapter 4 discusses the effect of thermal cycling on the mechanical and thermal properties of flat laminates. The results of microcrack evaluation on both flat laminates and sandwich panels are also covered.

Chapter 5 provides an overall conclusion on the topics discussed in the thesis. It also introduces some propositions for the future works.

Chapter 2: Literature Review

In this chapter, a review is carried out on the available references within the thesis scope. First, an overview of the polymeric matrix composites mostly used in space application is given with focus on carbon fiber reinforced polymer (CFRP) composite laminates. Next, out of autoclave (OOA) as the manufacturing method of choice along with its advantage and disadvantages over other techniques is described. Then microscopic evaluation of damages in CFRP due to thermal cycling is presented. Finally, the effect of thermal cycling on the mechanical and thermal properties of CFRP is reviewed.

2.1. Polymeric matrix composite materials used in space

Polymer matrix composites, and in particular continuous fiber reinforced polymer composites, have attracted tremendous attention from industries and research communities due to their improved properties to replace their metallic counterparts. Continuous fiber reinforced polymer composites can be categorized in two groups based on the matrix material; thermoset matrix composites and thermoplastic matrix composites. Thermoplastics become fluid when exposed to heat and solidify upon cooling. When thermoplastic is heated, no cross-linking within the polymer takes place. Thus, curing process is reversible which allows recycling of the material. Conversely, thermoset plastics are synthesized through cross-linking of polymer chains together

during a curing process. Curing process creates irreversible chemical bonds which prevents re-melting when thermoset polymer is exposed to heat. Therefore, thermosets are ideal for high temperature applications in both structural and sub-structural components, such as space applications, missile airframes, and supersonic aircrafts.

There are five main types of resins that are widely used in space: epoxy, polyimide, bismaleimides (BMI), phenolic and cyanate ster. The most common used resins in the advance composite materials market is epoxy. They offer excellent mechanical properties such as high strength as well as good physical properties such as low shrinkage, and excellent adhesion to various substrates and fibers. They also provide effective electrical insulation, chemical and solvent resistance, low cost, low toxicity and good dimensional stability. Due to their ease of processing, epoxies are of special interest to the industries. However, the temperature range that epoxies can be used is from room temperature to a maximum of 180 °C [17]-[19].

Bismaleimides (BMI) resins are able to go to higher temperature of up to 250 °C. Engine inlets, high speed aircraft flight surfaces are some examples of BMI applications. Other than excellent high temperature properties, BMI resins exhibit a good balance of electrical, mechanical, and thermal behavior; they can be easily processed, have nearly constant electrical properties and flame resistance. The only disadvantage of BMI resins is their extreme brittleness [17], [18]. When operation at higher temperatures (250 to 300°C) is needed, polyimides are useful due to their good durability at these temperatures [19].

Phenolics are another group of resins which have good heat and flame resistance and low processing cost; however, due to their brittleness they cannot be used as an alternative to epoxies and polyimides. These features make phenolics applicable just in non-structural components, especially in thermo-structural applications. Poor shelf life and high pressure cure are other shortcomings of this resin [18].

Cyanate ester resin is a category of thermoset resins which possess the properties of all other four resins as well as high glass transition temperature (250–290 °C), low moisture absorption, good dielectric properties and high toughness. However, they have high

processing cost in comparison with other resins. Table 2-1 lists some main properties of these polymer resins [17], [18].

Table 2-1 Comparison of common high performance thermosetting polymer matrices [18]-[21].

Property	**Epoxy**	**Phenolic**	**BMI**	**Cyanate ester**	**Polyimide**
Use temperature (°C)	RT–180	200–250	~200	~200	250–300
Cure temperature (°C)	RT–180	150–190	220–300	180–250	<100 °C
TGA onset (°C)	260–340	300–360	360–400	400–420	300–380
Tensile Modulus (MPa) × 10^{-3}	3.1–3.8	3–5	3.4–4.1	3.1–3.4	1.5–3
Density (kg.m^{-3}) ×10^{-3}	1.2–0.25	1.24–0.32	1.2–0.3	1.1–0.35	1.42
Cost (£/kg)	£20/kg	£2–4/kg	>£50/kg	£40/kg	>£80/kg

In early satellites in 1980s and 1990s, epoxy and cyanate were the material of choice for many components. As can be seen in table 2-2, epoxy as the resin was combined with carbon, fiberglass, aramid, Kevlar, graphite, and boron to make several subcomponents such as antenna support, antenna reflector, solar panel, solar yok, etc. in different spacecrafts [2].

Table 2-2 Application of advanced composites in different spacecraft components[*]

Spacecraft	**Years**	**Earliest use of specific composite components**
Intelsat IV [10 S/C]	1971±1979	Hybrid boron and fiberglass–epoxy aluminum foil waveguide; carbon–epoxy stiffeners on horn antenna support structure
Apollo [3 S/C]	1971±1972	Boron–epoxy lunar surface drill
ANIK B [3 S/C]	1972±1975	Carbon–epoxy mesh grid offset parabolic antenna reflector
Explorer	1973	Boron–epoxy booms
AST–6 (F/G)	1974	Carbon–epoxy antenna feeds support truss
SATCOM	1974±1975	Aramid/epoxy antenna reflector assemblies
Viking [2 S/C]	1975	Carbon–epoxy sandwich parabolic antenna reflector Carbon–epoxy boom
NATO 111 [3 S/C]	1976±1978	Carbon–epoxy cooler cover Aramid/epoxy antenna platform support cone
Voyager [2 S/C]	1977	Carbon–epoxy parabolic reflector Aramid/epoxy dichroic subreflector
SEASAT–A	1978	Carbon–epoxy rib stiffened reflector
HEAO 2	1978	Carbon–epoxy X–ray telescope optical bench
Ayame (ECS)[2 S/C]	1979±1980	Carbon–epoxy central cylinder Kevlar–epoxy solar array
FLTSATCOM [7 S/C]	1978±1986	Carbon–epoxy antenna deployment boom Aramid ground plane support

INTELSAT V [8 S/C]	1980±1985	2.0 and 1.0 in. diameter graphite/epoxy tube truss for antenna feed Copper coated low modulus carbon/epoxy waveguide Graphite/epoxy sandwich solar panel Low modulus carbon/epoxy solar array yoke
GOES [4 S/C]	1980±1987	Carbon–epoxy cooler cover; sandwich support beam
TDRSS [8 S/C]	1985±1995	8-foot–long carbon/epoxy antenna ribs (18 tapered tubes (1.6±1.0º)) Quartz fiber/epoxy radome
Hubble Space Telescope	1990	Carbon/aluminum high gain antenna mast 16-foot carbon/epoxy metering truss structure Carbon/epoxy truss tube focal plane array Carbon/epoxy optical bench for camera assembly
Clementine	1994	Graphite/epoxy interstage
Milstar [2 S/C]	1994	Graphite/epoxy sandwich upper platform for spot beam antenna Aramid/epoxy sandwich lens support structure. Low modulus carbon/epoxy corner fittings
INTELSAT VII [4 S/C]	1994±1995	High thermal conductivity graphite parts. Carbon/cyanate ester thrust tube
STEP 3	1 995	High modulus graphite/cyanate ester solar array substrates with three 0.06 mm plies)
AXAF ªChandraº	1999	High modulus graphite/cyanate ester solar array substrates and optical bench
Mars Mission Spacecraft and Stardust	1996±1999	High modulus graphite/cyanate ester bus structure Carbon-carbon engine shield Low modulus carbon±carbon thermal doublers High thermal conductivity graphite/cyanante ester battery support and radiator

[*] *Table adapted from Ref [2].*

2.2. Out of autoclave (OOA) manufacturing for space structures

Another influential factor in composite material properties is manufacturing method. Composite structures are often cured in an autoclave to achieve the required space grade quality. Figure 2-1 demonstrate a schematic of autoclave manufacturing technique. However, curing large structures needs access to large autoclaves which is limited and expensive. So, fabrication of large structures using OOA prepreg materials will result in huge amount of savings in manufacturing costs [22]. Figure 2-1 shows the schematics of both techniques. In OOA manufacturing method, presence of voids has been an issue due to lack of high pressure onto the laminate to eliminate the voids. As an alternative, a

vacuum pump is utilized to exert a low pressure for minimizing the void content [23]. With the aid of vacuum and high temperature in OOA technique a flawless part is manufactured and there is no need for the additional pressure source used in the expensive autoclave technique. By using a smaller portable oven, the desired temperature and vacuum can be achieved by a much lower cost than that of an autoclave and as a result producing a part with a lower overall cost is easily achievable.

Special prepregs are utilized in the OOA manufacturing technique that ease the removal of the trapped air during the hand layup procedure. Such prepregs are partially impregnated which forms a porous medium. When the resin changes into liquid and infuses into the fiber, the porous medium eases the removal of trapped air [24].

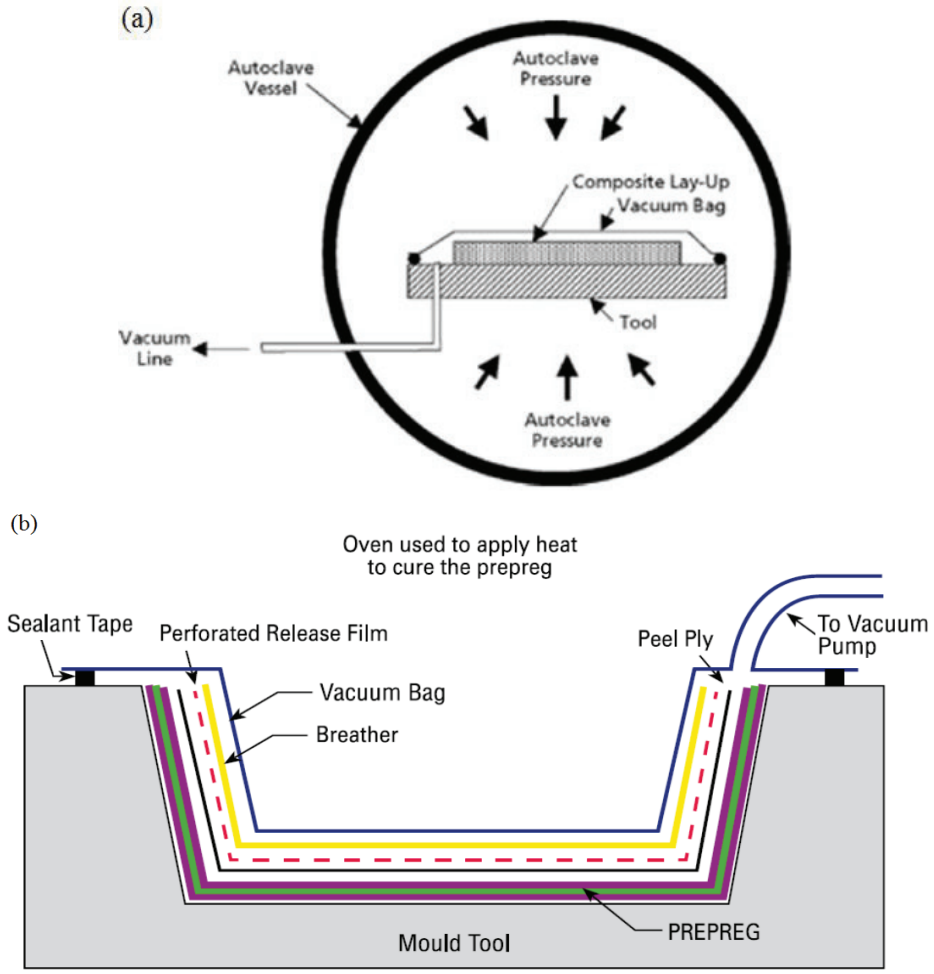

Figure 2-1 Schematic of: (a) autoclave; and (b) out of autoclave composite manufacturing. Both figures reproduced from Ref. [25].

OOA manufacturing technique has been widely studied in the literature and its advantages over autoclave technique for space applications has been discussed. Particularly, many researchers have used CYCOM 5320-1 which is a popular OOA carbon/epoxy prepreg for aerospace applications. Grimsley *et al.* [26] examined the compression performance of a heavy lift space launch structure manufactured using OOA. It was found that the properties of angel ply carbon/epoxy laminates fabricated with the OOA prepregs (T40-800b/5320-1) are the same as those fabricated with autoclave prepregs (IM7/977-3). He recommended the OOA technique to be considered as the robust alternative technique to autoclave to reduce the manufacturing cost for space structures.

In a technical report by Sutter *et al.* [27] for NASA, unidirectional OOA prepregs (IM7/MTM45-1 and T40-800b/5320) were compared with autoclave materials (IM7/977-3 and IM7/8552-1) for the application in heavy lift launch structures. Properties examined were short beam shear strength, compression strength, and open hole compression strength. They also examined the out-time effect on the mechanical performance by testing fresh laminates which were manufactured right after thawing and then comparing with those which were manufactured with prepregs remained out longer than out-life time specified by the vendor. OOA prepregs exhibited equal properties as their autoclave counterparts when made of fresh prepregs, but very sensitive to out-life time by showing high void content and decreased mechanical properties.

Even though laminates with low porosity have been successfully manufactured using OOA by many researchers, sandwich panels made by OOA method have not possessed as good quality as autoclave counterparts. For example, Chiou and Oldroyd [28] reported a high level of porosity in the bottom face sheet of OOA honeycomb structures. Carbon OOA prepreg in a sandwich structure held a lower fiber volume fraction compared with autoclave prepregs, and the curing process resulted in weight gain in the part.

Cauberghs *et al.* [29] studied the OOA manufacturing of aerospace representative parts with complex shape using carbon/epoxy prepreg technology and compared them with autoclave parts. CYCOM5276-1 plain weave was used to make the autoclave part and CYCOM5320 plain weave and MTM45-1 five harness satin (5HS) were used to fabricate OOA parts. The mechanical performance of OOA prepregs including compression and

bending properties were comparable to autoclave prepregs and both techniques yielded to void-free parts. OOA prepregs showed a higher glass transition temperature T_g compared with the autoclave prepreg. Achieving uniformity of thickness in the tight corners was reported to be challenging for both techniques.

Madhok [30]used CYCOM 5320-1 to identify the mechanical properties of the laminates made by automated fiber placement (AFP) to examine the effect of external pressure during curing. Results of mechanical tests such as the tensile, shear and compressive properties showed no significant difference between the laminates made with or without presence of external pressure. Mechanical properties of autoclave cured parts were slightly higher than the OOA ones. Also, the microscopic evaluation of both autoclave and OOA samples resulted in images with not much difference.

Based on this review on OOA manufacturing, void formation is an inherent characteristic of OOA composites which reduces the properties; however, some precautions are recommended to follow during manufacturing in order to reduce the void content and reach better properties. Therefore, OOA may results in manufacturing of composite laminates with comparable properties to their autoclave counterparts, suitable for space applications.

2.3. Microscopic Evaluation

To better evaluate and understand the thermal cycling effect on the composite materials, the damage resulted from cycling should be determined and analyzed. Several researchers have focused on this matter using different methods. A common approach is microscopic evaluation of the sample edges that could be done using optical microscopes or scanning electron microscope (SEM) [15], [16], [31]-[34].

The most frequent types of damage observed in composites were [35], [36]:

- microcrack formation,
- fiber/matrix debonding,
- and delamination.

For example, in a study by Adams *et al.* [37] on the thermal cycling effect on carbon/epoxy composites, delaminations were observed at the end of existing microcracks.

One of the important criteria concerning the thermal cycling effect on composites is crack development as a function of number of cycles. Herakovich and Hyer [36] examined the formation of microcracks as a function of thermal cycle numbers on the cross-ply graphite/epoxy composites. They found that the microcrack density increases by increasing the number of thermal cycles, reaching a saturation after certain number of cycles. Moreover, the presence of transverse cracks significantly reduced the laminate CTE. Henaff-Gardin *et al.* [38] also observed this saturation phenomenon in T300/914 carbon/epoxy laminates exposed to thermal cycles from −50 °C to 150 °C. They observed that crack initiation occurs in both 0° and 90° plies, and after crack saturation in the laminates, delamination occurs at 0/90 interface along the crack.

Shimokawa *et al.* [15] studied the thermal cycling effect on the carbon based polymer composites with quasi-isotropic pattern using two different matrix materials: 1) polyimide, 2) BMI. The cycles were run between −54 °C and 177 °C. For carbon/polyimide composites the microcracks formed only after 10 cycles while for carbon/BMI composites, microcracks appeared after 1500 cycles which indicates a higher resistance of BMI composite to thermal cycling in comparison with polyamide composite. For both laminates no microcrack saturation was observed even after 5000 thermal cycles. Figure 2-2 shows a typical transverse microcrack propagating from one layer to another after thermal cycling.

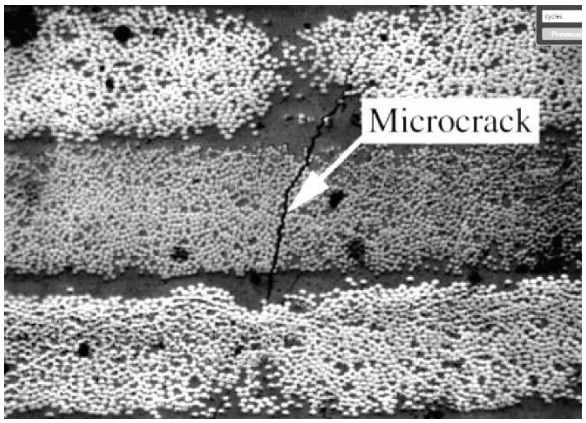

Figure 2-2 A typical transverse microcrack as a result of thermal cycling [15].

In another research conducted by Adams *et al.* [37] effect of thermal cycling on cross ply graphite epoxy laminates with different stacking sequences was investigated. Even though the crack density in all different laminate configurations increased with increasing thermal cycles, it was found that laminate configuration has a significant effect on the crack density as well as the temperature at which transverse cracking initiates. For example, in some laminates microcracks appeared only after one cooling cycle down to −45° C whereas for some others no microcrack was formed even after a cooling cycle down to −157° C. Some laminate configurations, such as $[90_3/0]_s$, were found to be less stable compared to other configurations when exposed to thermal cycling and exhibited out of plane warping. Moreover, no crack saturation was observed on neither of laminates even after 500 thermal cycles.

It could be also of interest to know in which ply through the thickness the damage would initiate. Based on some research works conducted by Bechel *et al*. [16], [32] - [33], outer plies in laminates are more susceptible to damage than inner plies. However, there are some evidences that disagree with this observation; *e.g.* Henaff-Gardin *et al.* [38] observed large microcrack densities in the inner plies of their laminates rather than outer plies.

2.4. Mechanical Properties

Since the mechanical properties establish the primary criteria for composite performance, measurement of such properties have been used widely to characterize the extent of damage upon exposure to different environments. As many composite structures are working at extremely low and/or high temperatures, the material properties at these temperatures are required for design purposes. The most important properties discussed in literature are strength and stiffness characteristics. Hence, the effect of extreme temperatures on these mechanical properties is reviewed in this section.

One of the important mechanical characterizations is the interlaminar shear strength (ILSS) in which the shear strength of matrix layer between adjacent plies is measured [39]. Even though exact determination of ILSS is not easily possible, its approximate values can be determined by different tests such as three-point bending of short beam

(Figure 2-3). Usually, a relatively thick unidirectional laminate with at least 16 plies is cut in a short beam size such that the fibers are along the beam axis (direction 1 in Figure 2-3) and then it is normally loaded along direction 3. If the beam is not thick enough and has less than 16 plies, there might be compressive failure at the loaded points (middle point or two corner points) and the ILSS results are not valid. A laminate with about 50 plies is recommended for getting more accurate results. Three-point bending is a relatively simple test method, which is also utilized for quality control purposes in lamination processes. It is also common test method in determination of matrix-dominated properties.

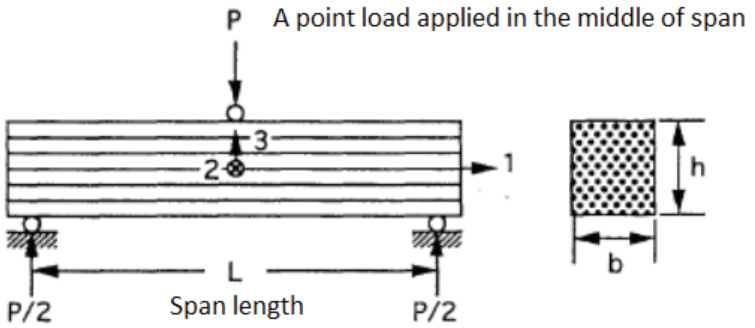

Figure 2-3 Three-point bending test of a short beam for measuring interlaminar shear strength (ILSS). Figure adapted from Ref [39].

It is known from classical beam theory that the maximum shear stress in this beam occurs in the midplane and the maximum normal stress due the bending occurs in the outer planes, which is compressive stress in top layer and tensile stress in bottom layer. For a short beam, the ratio of span length to thickness (*L/h*) is very small and thus the maximum stresses resulted from the bending moment at the outer layer is small compared to the shear stress due the shear load in the midplane. Therefore, a short beam in a three-point bending test can provide the approximate ILSS properties by having the failure happening in the midplane prior to flexural failure in the outer layers.

From classical beam theory, the shear stress at the midplane is given by

$$\tau_{\mathrm{ILSS}} = \frac{3}{4}\frac{P}{bh} \qquad \text{Equation (1)}$$

where

τ_{ILSS}: short beam strength (MPa);

P: maximum load observed during the test (N);

b: measured laminate width (mm);

h: measured laminate thickness (mm).

The following relationship must be checked before the ILSS testing in order to have shear failure occur prior to bending failure:

$$\frac{L}{h} < \frac{X_1}{2\tau_{\mathrm{ILSS}}} \qquad \text{Equation (2)}$$

in which

L: beam span length (m);

X_1: Flexural strength of beam in fiber direction (MPa).

There have been several investigations on the effect of thermal cycling on ILSS of composites. Particularly for satellite antenna application, Jianping *et al*. [7] studied the effects of thermal cycling on mechanical and physical properties of carbon/epoxy composites. They used M40J/BA204, which is a high performance carbon/epoxy system. Samples were thermal cycled for up to 200 cycles in a temperature range of −196˚C to +130˚C and variations in mechanical properties including longitudinal tensile properties, flexural properties and ILSS was measured. The longitudinal tensile properties of composite decreased significantly up to 100 thermal cycles and then leveled off with further cycling up to 200 cycles. The longitudinal flexure properties and ILSS were initially improved and then decreased to some extent with further cycling from 100 to 200 thermal cycles.

In another work, the effect of thermal cycling on physical and mechanical properties of unidirectional carbon/BMI composite laminates was investigated by Yu *et al* [11]. Composite samples were cycled between −140˚C and +140˚C up to 300 thermal cycles. Flexural strength and ILSS of the composite showed similar behavior; they firstly increased and then flatten off after 198 cycles. The transverse tensile strength dropped by about 9% and reaching a plateau after 95 cycles.

An attempt to emulate the effect of a space environment on IM7-977-2 carbon–epoxy specimens were made by Kessler *et al*. [40]. Test samples were subjected to thermal

cycles between −250 ˚C and +125˚C. The ultimate tensile strength was measured after 0, 2, 5, and 10 cycles. No significant change was observed in material tensile strength. Moreover, material properties of individual fibers were not affected in an unexpected way by the thermal shocking.

In another research work by Bechel *et al.* [33], IM7/5250-4 carbon/bismaleimide laminates were thermally cycled between extreme low temperature and room temperature and then tested for evaluation of tensile properties and microcrack propagation. Three different layups were tested: cross-ply in two configurations of $[0/90]_{2S}$ and $[(90/0)_2/\overline{90}]_S$ and also quasi-isotropic with $[0/45/-45/90]_S$ configuration. Thermal cycles were conducted for 400 cycles such that in each cycle the test sample was dipped in liquid nitrogen (LN_2) and then was exposed to room temperature. The longitudinal tensile strength was reduced by 8.5% for $[0/90]_{2S}$ and $[0/45/-45/90]_S$ layups while the longitudinal tensile modulus remained almost unaffected. Moreover, the microcrack in the outer plies was more severe than in the inner plies. It was also observed that between the two cross-ply laminates, $[0/90]_{2S}$ that had adjacent two plies of the same orientation in the middle was more prone to micro-cracking of the inner plies compared with $[(90/0)_2/\overline{90}]_S$ which exhibited no cracks in the inner plies.

Thermal cycling of 5HS laminates with $[0/45]_S$ configuration made of carbon/cyanate ester prepregs was studied by Ajaja and Barthelat [41]to examine the effect of microscopic damage on mechanical properties. Samples were exposed to thermal cycling in two different ways: the first method was extreme cycling in which samples were exposed to cold cycling by dipping quickly in liquid nitrogen (−210 °C) for 10 minutes and then transferred to room temperature water (+20 °C) for 5 minutes. In the second method, thermal cycling between +20 °C and −120 °C was performed in a DMA with a controlled temperature rate. A series of three point bending tests were also carried out on all samples, which demonstrated almost 50% reduction in bending stiffness after only five extreme cycles and the microcracks were detected too. However, the bending stiffness of samples cycled in DMA was not changed even after eight cycles and no microcracks were observed.

Dutta *et al.* [42] examined the influence of low temperature thermal cycling on the tensile properties of unidirectional and quasi-isotropic laminates made of first generation carbon/epoxy composite. Specimens were cycled up to 10 times between the liquid nitrogen temperature and room temperature. For unidirectional laminates, fiber dominated strength increased while matrix dominated strength decreased as a result of low temperature cycling, with no significant change in elastic modulus. In another study by Dutta [43] on low temperature behavior of graphite epoxy, it was shown that unidirectional tensile strength decreased, however, due to the matrix hardening, off-axis and transverse strength increased. Off-axis stiffness and strength showed degradation when exposed to prolonged thermal cycling though.

The effect of vacuum thermal cycles on the mechanical properties of unidirectional carbon fiber/epoxy laminates was studied by Park *et al.* [44]. The temperature range for cycles was between −175 °C and +120 °C under high vacuum state. After exposure to 2000 thermal cycles, longitudinal properties like tensile strength didn't change significantly (less than 10%). However, transverse properties like compressive strength and ILSS dropped by about 15%.

In a research work conducted by Shin *et al. [45]*, the mechanical properties of graphite/epoxy composites (HFG CU-125NS) exposed to simulated thermal cycling condition of satellite at low earth orbit were examined. The specimens were cycled up to 80 times between −70 °C and +100 °C. By increasing the number of thermal cycles, the stiffness and strength of the composite samples decreased with a higher reduction rate for transverse properties due to the matrix loss at the surface of the composite.

Shear stiffness dropped quickly by increase in the number of thermal cycles but not as rapid as flexural stiffness which decreased by 25% after exposure to 80 thermal cycles. The compressive and tensile stiffness variation was moderate.

Despite the stiffness response for this material to thermal cycling, a dramatic fall was observed in strength properties except ILSS which was not affected by thermal cycling. The largest change was found in transverse flexural strength for 34%. Generally, matrix dominated properties showed the highest reduction due to the thermal cracking.

Owens and Schofield [46] examined the behavior of $(0/90)_6$ and $(\pm45)_6$ laminates made of satin weave carbon/polyamide prepregs exposed to thermal cycling. Thermal cycles were between −18 °C and +232 °C temperature ranges with a heating and cooling rate of 43 °C/min and 10 °C/min, respectively. Microcracks were detected within the cross ply laminates after cycling but no degradation in longitudinal tensile properties was observed after exposure to 5000 cycles. Conversely, the $(\pm45)_6$ laminate was not affected after 3000 cycles, however, tensile strength dropped by 34% after 5000 cycles. It was also reported that laminate performance was more affected by the cracks in the inner plies and not the outer ones. Moreover, no saturation in damage was reported even after 5000 thermal cycles.

Gao *et al.* [47] studied the vacuum thermal cycling of unidirectional carbon/epoxy composite (M40J/AG-80) over the temperature range of −180 °C to +140 °C. After different number of thermal cycles, the composite mechanical properties including tensile strengths at fiber and matrix directions, bending strength, and ILSS were measured (Figure 2-4). The observations showed that both longitudinal and transverse tensile strengths decreased and reached a plateau after 48 and 40 cycles, respectively. The bending strength behaved differently such that it increased first up to 40 cycles and then decreased until it remained unchanged after 97 cycles. The trend for the ILSS was different; it dropped for the first few cycles by about 2% followed by an increase to a value of about 4% higher than the non-cycled strength value. Regardless of the first few cycles, in overall, the ILSS stayed constant compared to the tensile and bending strength. It was stated that ILSS strength was mainly related to the cross-linking density which would increase the shear strength of the resin.

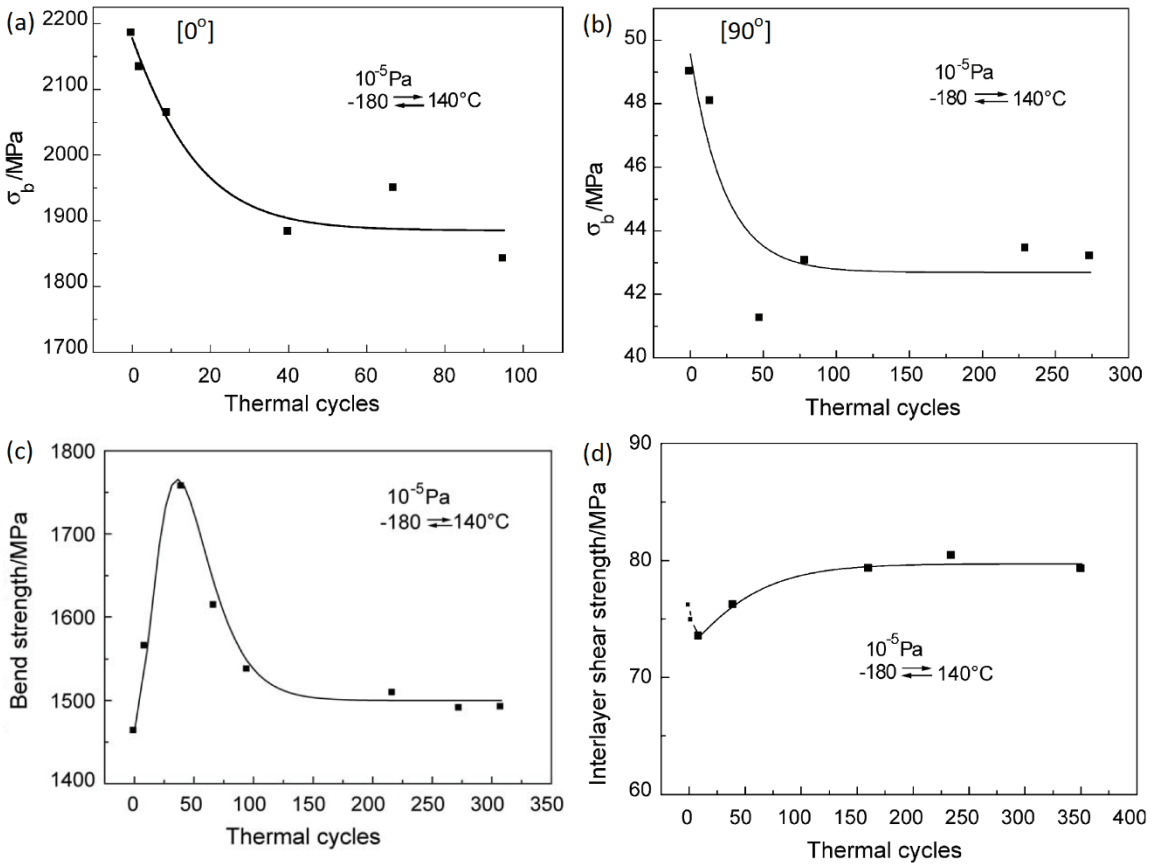

Figure 2-4 Mechanical properties of unidirectional M40J/AG-80 (carbon/epoxy composite) vs thermal cycles: (a) 0° tensile strength; (b) 90° tensile strength; (c) bending strength; (d) interlayer shear strength. All figures adapted from Ref [47].

2.5. Thermal Properties

In this section, thermal cycling effect on thermal properties is divided in two sections: thermal expansion characteristics and dynamical mechanical properties.

2.5.1. Effects of Thermal Cycling on Thermal Expansion characteristics

The basic building block of the most structural polymer composite laminates is a thin orthotropic lamina (ply) composed of parallel fibers embedded in a polymer matrix. Due to the far larger modulus of fiber compared with matrix, CTE of the lamina in fiber direction is more affected by the fiber CTE. Carbon fibers CTE in longitudinal and transverse direction is negative and positive, respectively, and polymer CTE is positive in all directions. Therefore, for carbon fiber reinforced composites, lamina CTE could be negative in fiber direction, but positive in transverse direction in an order of magnitude

larger than fiber direction. Since laminated composites are typically manufactured with different fiber orientations to meet specific design requirements, the overall laminate CTE is greatly dependent on the stacking sequence of constituent plies [48].

Composite materials in space encounter several thermal cycles during their life time. Particularly, for epoxy matrix reinforced with carbon fiber, due to the large difference of epoxy CTE and carbon CTE, thermal stresses are induced in the composite under cyclic temperature changes. Thermal stresses could cause interfacial debonding and matrix microcracking in the composite which finally results in material system failure [7].

Effect of temperature on the polymer CTE has been studied by several researchers. Yu *et al.* [11] investigated the effect of vacuum thermal cycling on the physical properties of carbon/BMI unidirectional laminate composites composed of 16 prepreg plies. They concluded that the changes in CTE is determined by the degree of interfacial debonding between fibers and matrix. For the initial 48 thermal cycles both transverse and longitudinal CTEs remained the same as the CTE of unexposed composites, indicating that the thermal cycling exposure had no significant influence on the formation of debonds at fiber/matrix interface up to 48 thermal cycles. With increasing thermal cycles, the constraints between fibers and matrix are decreased due to a rise in interfacial debonding, which resulted in a gentle increase in transverse CTE of the composite exposed to temperature changes. On the other hand, the longitudinal CTE of the composite at the beginning of cycling was fiber dominated due to good bonding at matrix/fiber interface which resulted in negative CTE. By further cycling and continuing up to 283 cycles, interfacial debonding increased and longitudinal CTE became matrix dominated which resulted in positive CTE.

Recently, Ajaja and Barthelat [41] have studied the effect of thermal cycling on the CTE of carbon fiber reinforced cyanate ester composites. Samples of 0.5 mm thickness were exposed to 16 thermal cycles with temperatures varying from −70 °C to +150 °C using a thermomechanical analyzer (TMA). Their results are in agree with Tompkins results [49] where no variation in CTE was observed for woven composite materials.

Shin *et al.* [45] evaluated the changes in the CTE of the graphite/epoxy unidirectional composites fabricated from prepreg tapes in autoclave. They examined the CTE

variations in three directions (longitudinal, transverse and thickness-direction). In their experiments, one thermal cycle was defined from −70 °C to +100 °C and back to −70 °C in a period of about 90–95 min. As can be seen from Figure 2-5, their results indicated that CTE is dependent on the temperature and also is affected by the thermal cycling; with increasing thermal cycles, the CTE of composite at a given temperature decreased in all three directions. They concluded that the reduction in CTE was mainly due to matrix loss caused by thermal cycles. Since fiber volume fraction increases by matrix loss, and higher fiber volume fraction means fiber dominated properties, therefore matrix loss leads to the CTE reduction.

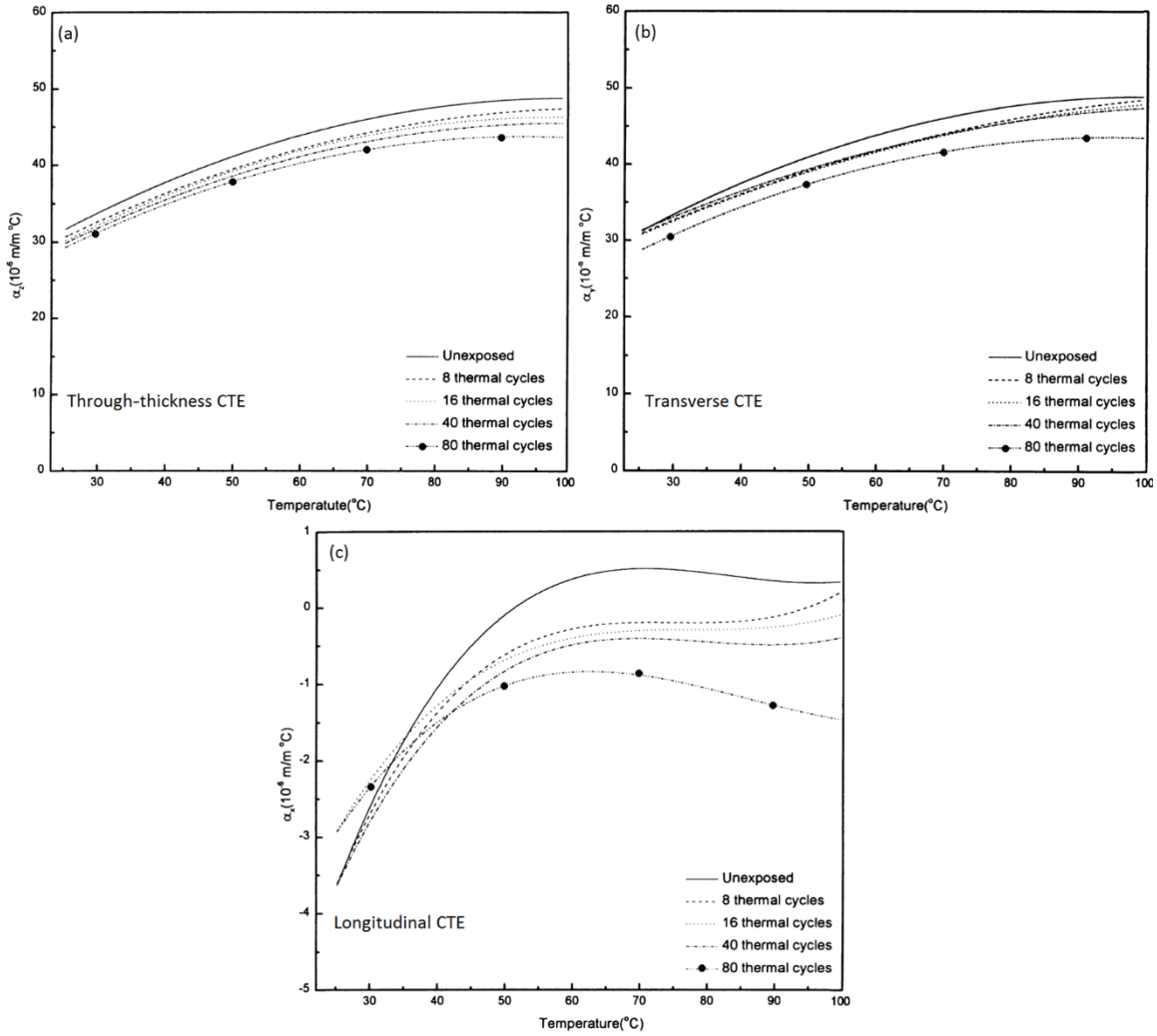

Figure 2-5 Changes in CTE of the graphite/epoxy unidirectional composites fabricated from prepreg tapes in autoclave exposed to thermal cycling from −70 °C to +100 °C: (a) Through-the-thickness CTE; (b)Transverse CTE; (c) Longitudinal CTE. All figures adapted from Ref [45] with some modifications.

The effect of thermal cycling on longitudinal CTE of symmetric cross ply composites made of thin and thick epoxy/graphite prepreg plies (P75/ERL 1962) was studied by Tompkins *et al.* [50]. All of the laminates were thermally cycled between −156 °C and +121 °C up to 1500 times. CTE of laminate made of thin plies stayed unaffected up to 500 cycles, in contrast to the laminate with thick plies whose CTE dropped significantly from the early cycles. With increasing the number of cycles to 1500, a drop in the CTE of laminates with thin plies was also observed.

In another study conducted by Gao *et al.* [47] on the thermal cycling of unidirectional carbon/epoxy composite (M40J/AG-80), the transverse CTE variation before and after thermal cycles in the range of −180 °C to +140 °C was quite small. However, the behavior for longitudinal CTE was different; before cycles it was negative and after 315 cycles it changed to a nonlinear behavior such that it was decreased to a much smaller negative CTE value at temperatures below zero and a positive CTE at temperatures above zero. They inferred that the changes in the longitudinal CTE was related to the interfacial debonding extent, while the variations in transverse CTE was mainly due the increase in cross-linking density in the epoxy matrix.

2.5.2. Effects of Thermal Cycling on Dynamic Mechanical characteristics

T_g is a temperature above which the polymer behavior changes from glassy to rubbery with significant drop in stiffness and enhance in viscosity. Effect of thermal cycling on glass transition temperature (T_g) and damping properties of the polymer composites studied by some other researchers is reviewed in this section.

Jianping *et al*. [7] studied the effects of thermal cycling on the T_g of a high performance carbon/epoxy composite (M40J/BA204) for satellite antenna. Samples were exposed to 200 thermal cycles from −196˚C to +130˚C and T_g was measured using a dynamic mechanical analyzer (DMA). DMA results showed that T_g increased at the initial stages of the cycling and then decreased gradually after 100 thermal cycles. They concluded that the material cure was not complete so the heating effect of the thermal cycling caused more cross linking of the resin matrix which led to a higher T_g. After improving the cross linking degree to some extent, further cycling caused microcrack formation due to the CTE mismatch between the fibers and matrix resulting in a decrease in T_g of the

composites. Several other researchers [11], [44], [47], [51] studied the effect of thermal cycling on the Tg and observed the same results as the Jianping results.

Wang *et al.* [52] evaluated the effect of cryogenic environment on damping properties of unidirectional carbon fiber reinforced bismaleimide composite (T700/6421 BMI composite). The specimens were soaked in liquid nitrogen in six different groups for 1, 10, 20, 50, 80 and 100 days and then tested in DMA machine to measure their T_g and loss factor (tan δ) as a function of temperature. Figure 2-6 shows the loss factor peaks for their experiment. By increasing the soaking time, both T_g and tan δ increased, indicating more energy dissipation due to fiber/ matrix debonding. They inferred that the CTE mismatch between fiber and matrix introduces thermal residual stresses, leading to fiber/matrix debonding by increasing the dipping time in liquid nitrogen.

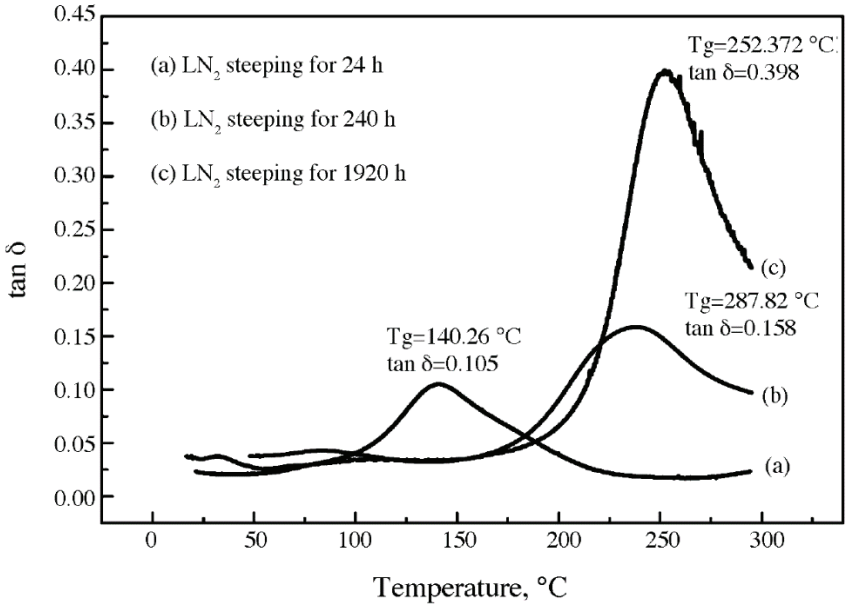

Figure 2-6 Effect of cold environment on damping properties, figure adapted from Ref [52].

Chapter 3: Experimental

In this chapter, the details on the selected OOA prepreg materials, employed manufacturing technique, sample preparation, thermal cycling procedure and equipment, and all other required equipment for thermal and mechanical characterizations of composite samples are described.

3.1. Materials Selection

The material used for this project was Cycom 5320-1 manufactured by Cytec Engineered Materials Inc. which is a composite material system for manufacturing of primary structural parts in today's aerospace industry [53]. It is a toughened epoxy prepreg system specifically designed for OOA manufacturing. Two different styled composites made up of this material were used for the analysis: a unidirectional (UD) composite and a woven fabric (5-harness carbon/epoxy satin prepreg or 5HS). The purpose of selecting two different styled composites was to examine and compare their mechanical and thermal performance after being exposed to thermal cycling. The samples were manufactured from the same resin system provided by Cytec and with same total laminate thickness of ~3.5 mm to have results that are more comparable. Table 3-1 summarizes the material properties of the prepregs used in this thesis and Figure 3-1 shows the two prepreg materials.

In addition to these two materials, a sandwich panel with honeycomb core composed of Kevlar (1/4" core thickness) was also studied in this research to analyze the effect of thermal cycling on the performance of adhesive between skin and core in the sandwich panel. This sandwich panel was provided by the MDA Corporation and no further information on its properties was released (Figure 3-2).

Table 3-1 Material properties of the prepregs used in the current research [54].

Property	**UD OOA**	**5HS OOA**
Manufacturer	Cytec Materials	Cytec Materials
Fiber	T650-UD carbon	T650-5HS carbon
Resin	Cycom 5320	Cycom 5320
Tow count (fiber/tow)	Nil	6000
Yarn width (mm)	Nil	2.03
Areal density (g/m2)	882.34	1178.62
Resin content (%)	36	36

(a) (b)

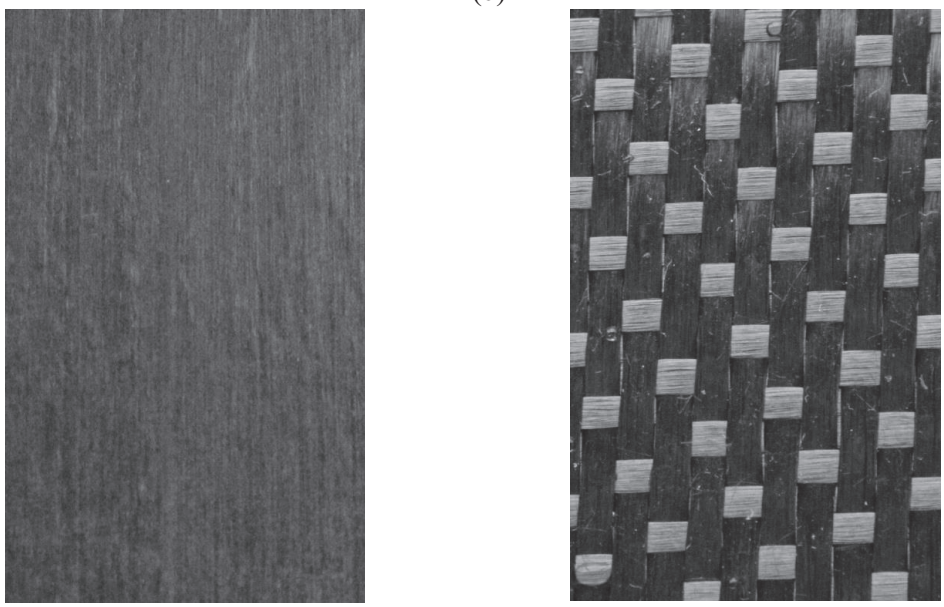

Figure 3-1 Cycom 5320-1 Prepreg: (a) unidirectional tape, (b) 5-Harness woven [54].

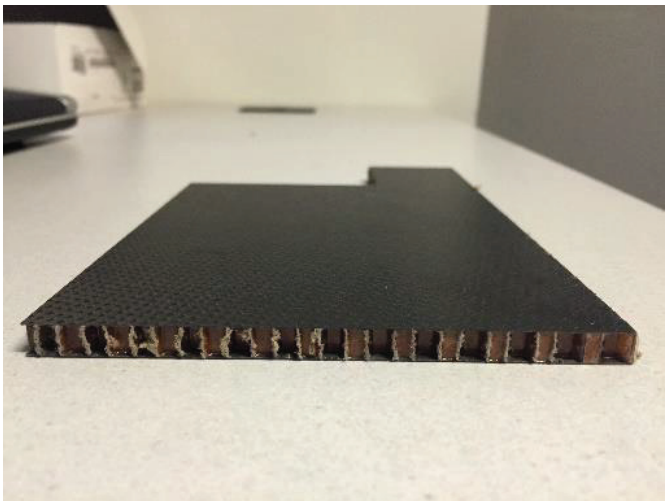

Figure 3-2 Sandwich panel provided by MDA Co.

3.2. Manufacturing of the OOA Sample

This section explains the steps in manufacturing the composite plates. Two different laminates were made:

Laminate 1: A 24-layer unidirectional laminate with 152.4 mm × 152.4 mm dimensions made of unidirectional tape;

Laminate 2: An 8-layer cross-ply laminate with 380 mm × 380 mm dimensions made of 5HS woven fabric.

The plate was manufactured by the hand layup method and cured inside the oven.

3.2.1. Layup Procedure

The schematic of vacuum bag is shown in Figure 3-3. The hand layup procedure was followed according to the steps below [55]:

I: The prepregs were cut into the required dimensions. In order to improve prepregs tackiness, they were left at room temperature for one hour after cutting.

II: To improve the surface finish of the final plate, the mold surface was first cleaned with acetone. To facilitate the demolding process, a thin layer of release agent was applied to the mold surface and waited for it to dry for 10 minutes. Afterwards, the prepregs were stacked up one on top of the other. To eliminate the air trapped between the layers and reduce the void content as

much as possible, a roller was used to apply pressure on each layer. Roller also increases the adhesion of adjacent layers as well. With the aid of vacuum pump, debulking was performed every four layers to eliminate wrinkles and voids.

III: To track the plate temperature during the curing process and afterwards during the thermal cycling process, a k-type thermocouple was bonded to the edge of the mid plane of the laminate. Since the carbon fibers are conductive and cause false temperature reading, a release film was utilized to avoid the contact between the prepreg and the thermocouple wire.

IV: After the layup was complete, one layer of barrier film was applied. Then, the whole surface was covered with a breather cloth, making sure that the breather reached the vacuum ports (the breather under vacuum ports was doubled). Subsequently, using a vacuum bag the mold was covered and its edges were sealed by sealant tapes. Finally, the plate was vacuumed at a pressure of 0.1 MPa for one hour to eliminate the entrapped air and moisture.

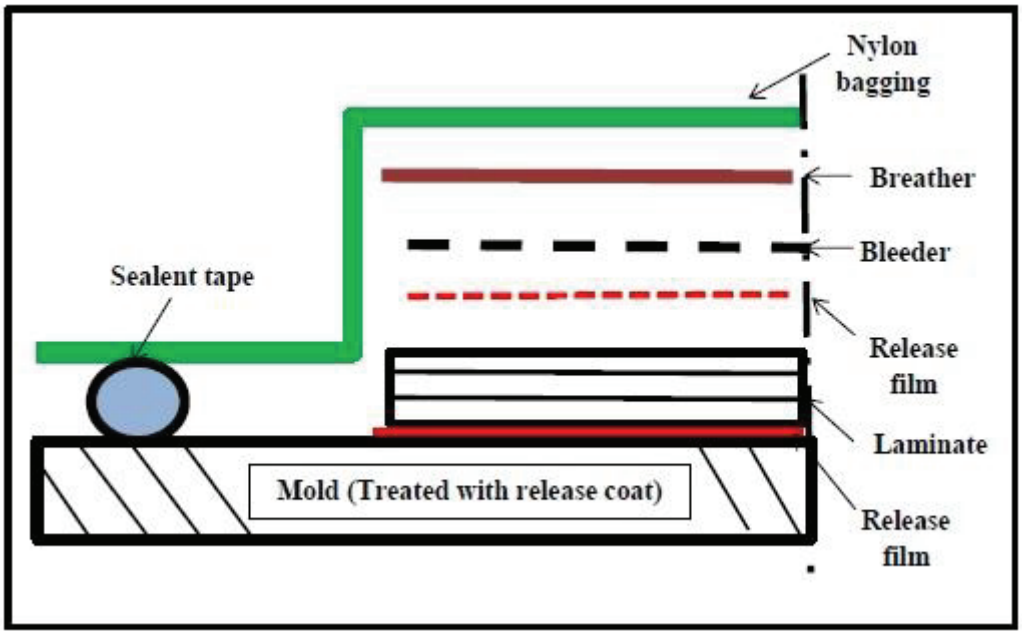

Figure 3-3 Schematic of vacuum bag [56]

3.2.2. Curing process and curing cycle

To cure the composite laminate, the cure cycle recommended by the manufacturer for Cycom 5320-1 material system was used to cure the composite laminates [53]. The material was cured in a forced air circulation oven shown in Figure 3-4. A vacuum pump was used to pull the vacuum on the layup. In order to more accurately measure the laminate temperature during the cure and avoid the temperature delay between the oven temperature and plate temperature, the other end of the thermocouple already embedded in the laminate mid-plane was taken out of the oven using a data acquisition system. It was assumed that once the center ply of the laminate was within ±5 °C of the desired temperature, all plies of the laminate had reached temperature equilibrium.

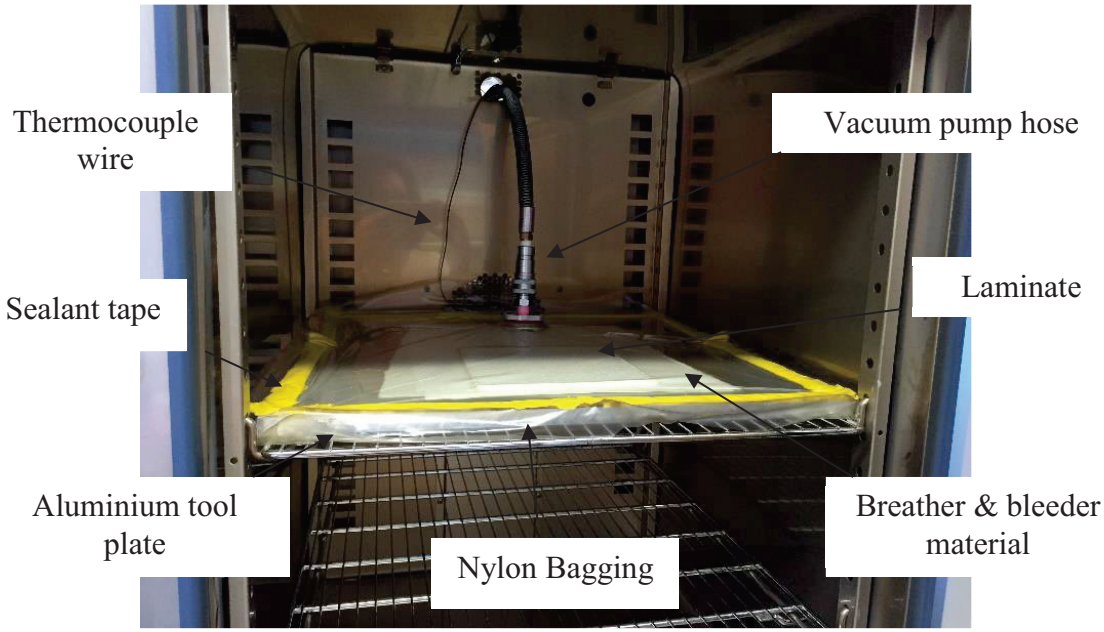

Figure 3-4 Air forced circulation oven used for curing laminate and thermal cycling.

Figure 3-5 shows the cure program for the composite plate. As shown in this figure, the oven temperature was ramped from the room temperature to 120 °C and hold at this temperature for 3 hours to cure the epoxy. Then it was raised to 177 °C and kept for 2 hours for the post-curing, and finally the temperature was allowed to fall down to room temperature. All the temperature changes occurred at a ramp rate of 0.6–2.8 °C/min. One fabric plate and two UD plates were fabricated for this research. The manufactured UD plate and 5HS plate are shown in Figure 3-6.

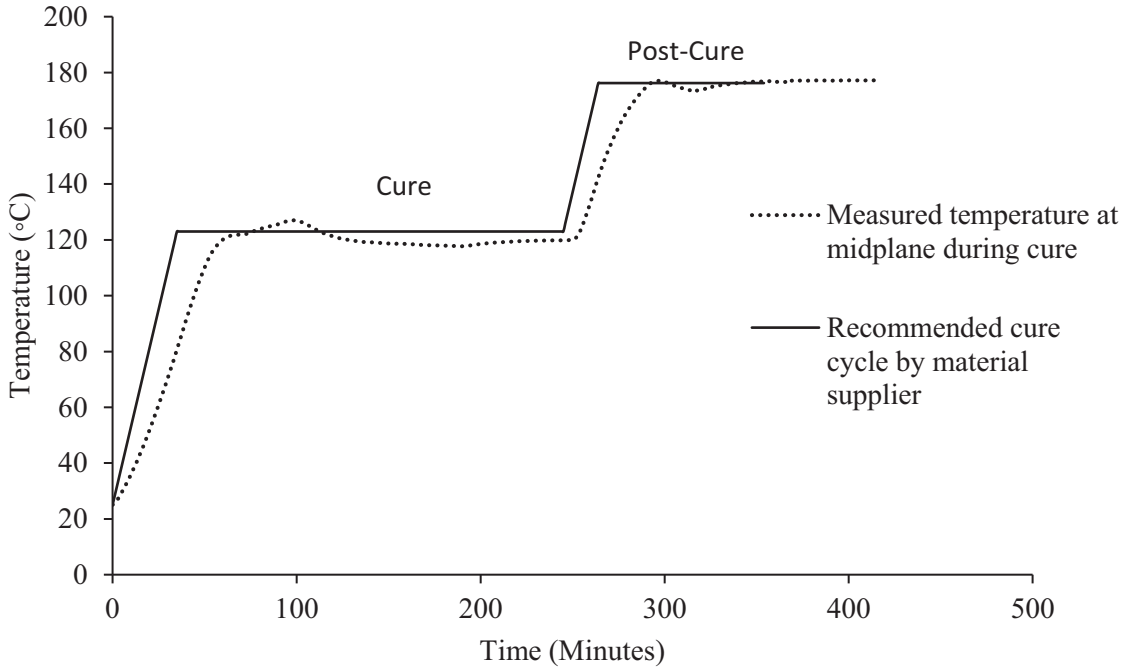

Figure 3-5 Cycom 5320-1 cure cycle: experimental and recommended cycles match very well.

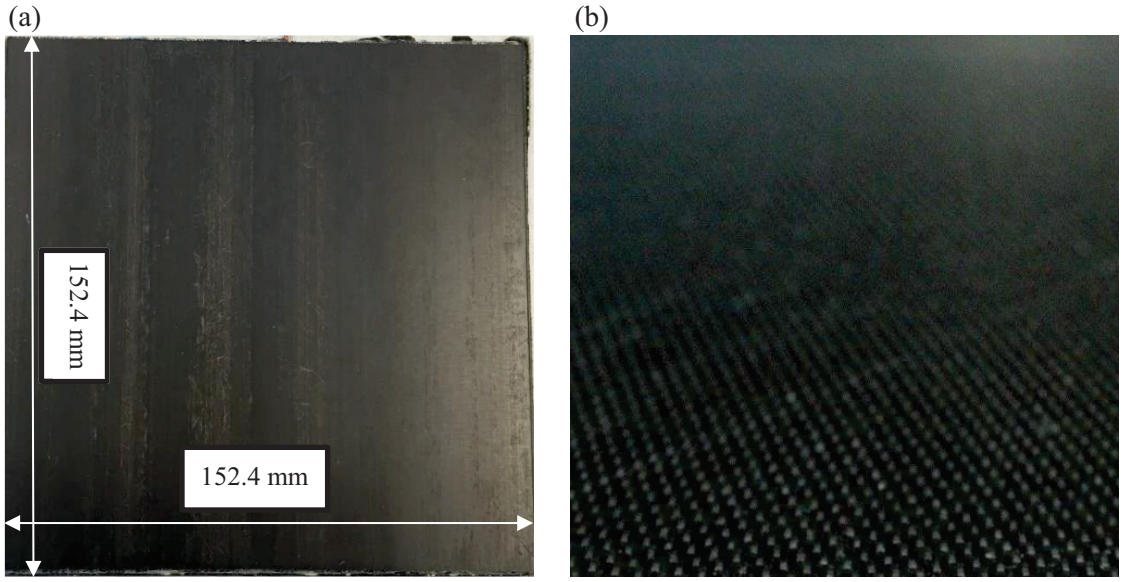

Figure 3-6. Initial sample made by hand layup process using: (a) complete plate made of Cycom-5320 UD; (b) partial image of Cycom-5320 5HS.

3.2.3. Composite laminates degree of cure

After the curing process is complete and the plates are cooled down to room temperature, the molds are taken out of the oven and laminates are removed from the mold. To find

out the laminates degree of cure, a differential scanning calorimetry (DSC) test was run. DSC is a thermo-analytical based technique in which the heat difference to elevate sample temperature compared with a reference material is measured with respect to a temperature range. The heat flow of raw prepreg and cured laminates was measured using a TA Instrument Q200 DSC machine (Figure 3-7). A temperature ramp from 25 °C to 300 °C at 10 °C/min was run to obtain the total heat of reaction of the raw prepregs and cured laminates. The degree of cure (α) ranges from 0 for completely uncured to 100 for fully cured and can be calculated using the formula below:

$$\alpha = \left(1 - \frac{\text{residual heat } (\frac{\text{J}}{\text{g}})}{\text{total heat of reaction } (\frac{\text{J}}{\text{g}})}\right) \times 100$$

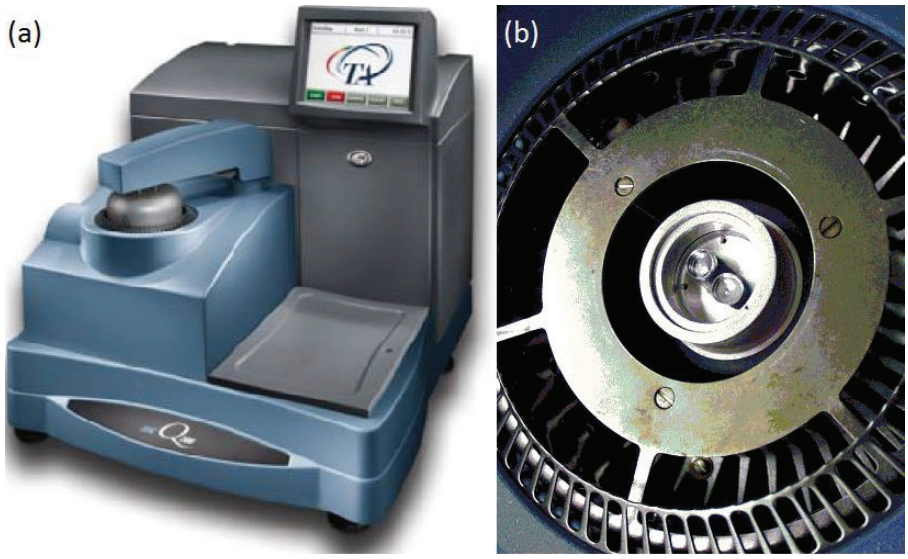

Figure 3-7 (a) TA instrument Q200 DSC machine; (b) Sample and reference platform inside DSC [57]-[58].

3.3. Sample Preparation

The laminate edges were trimmed about 25 mm from each side. Then samples were cut from the plate according to the coupon size of the different tests, including ILSS, CTE, DAM, and microscopy. The coupon dimensions were chosen based on the standard requirements for each specific test. Table 3-2 lists the sample size and size guide for each individual test. A circular diamond saw with continuous flow of water for cooling was used to cut the samples.

For optical microscopy of samples, a good quality of the surface was required. One specimen from each laminate prior to cycling was polished on two sides of the cross section such that the fibers were perpendicular and parallel to the polished edge. The samples were gradually polished with grinding papers No. 300, 600, and 800 on a rotating polish machine (Mecatech 234). For a better microscopy observation, best effort was made to ensure the specimen surface is not inclined during the polishing. However, for sandwich panel samples, obtaining a good quality polished surface was not possible due to the damage to the core during polishing.

Table 3-2 Required sample size and number for different tests according to the standard requirements

	Test			
	ILSS	**CTE**	**DMA**	**Microscopy**
Sample width (mm)	6.5	5	15	10
Sample Length (mm)	20	10	50	20
Number of specimens per set	5	5	2	1
Size Guide	ASTM D2344	ASTM E831	DMA Manual, TA Instruments	N/A

3.4. Thermal Cycling

Five different sets of samples were cycled at 30, 60, 100,150 and 200 times, and compared with one set of unexposed samples (non-cycled). A complete cycle was defined as 2 min in the liquid nitrogen (LN) at −196 °C, 5 min at room temperature (RT) of +23 °C, 10 min inside the oven at +140 °C, and 5 min again at RT. Thus, the total time for one cycle was 22 minutes.

To have a control specimen for thermal cycling, one sample was cut from the laminate such that the thermocouple embedded in the laminate during manufacturing step was inside the cut sample. The time necessary for the center ply of this control specimen to reach the required hold temperatures (within ±5 °C of the target temperature) was recorded for each step of the thermal cycle. Figure 3-8 shows the temperature cycle measured using a control specimen.

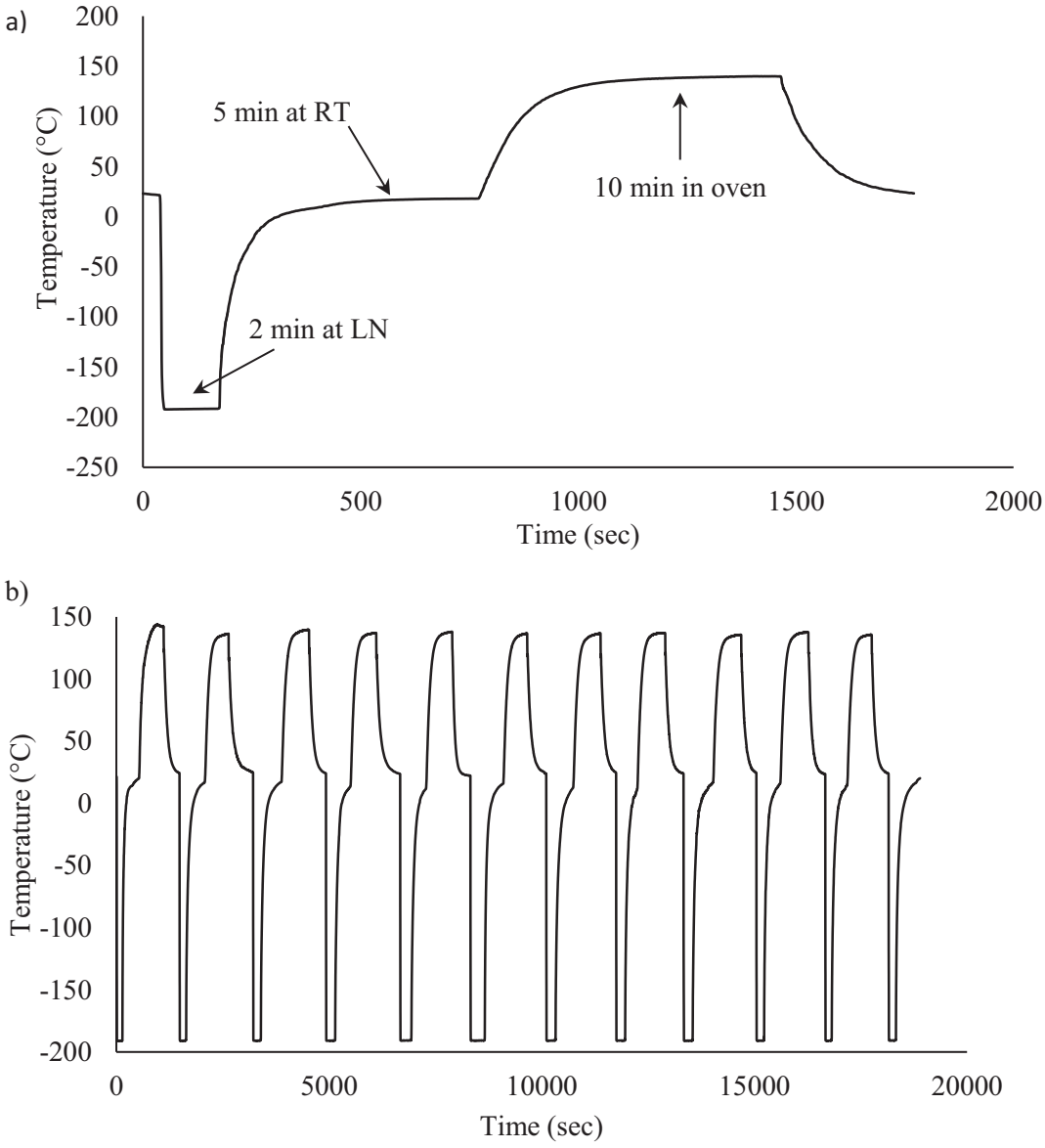

Figure 3-8 Temperature cycle vs. time for a) one complete cycle and b) ten cycles. Required time to stay at the room temperature (RT) of +23 °C, in the liquid nitrogen (LN) at −196 °C, and inside the oven at +140 °C is shown.

Setup: Cycling of the coupon samples was performed in a jar containing liquid nitrogen (LN) for cooling phase and inside a convection oven for heating phase. Figure 3-9 shows the thermal cycling setup. The specimens were placed in a basket made of metal wire mesh having different shelves to minimize the contact between them and make the specimen temperature equilibrium faster. The basket was immersed in LN bath for

cooling phase and put in the preheated convection oven for the heating phase of the cycle. After each cooling and heating phase, the basket containing the specimens was placed in RT to reach ambient temperature. Temperature cycle vs. time was recorded for several cycles using the control specimen (Figure 3-8).

Microscopy: Some samples were needed for the purpose of crack investigation using optical microscope. Those samples were analyzed every one cycle to check the crack initiation and propagation during the first 10 cycles, and afterwards they were analyzed every 10 cycles.

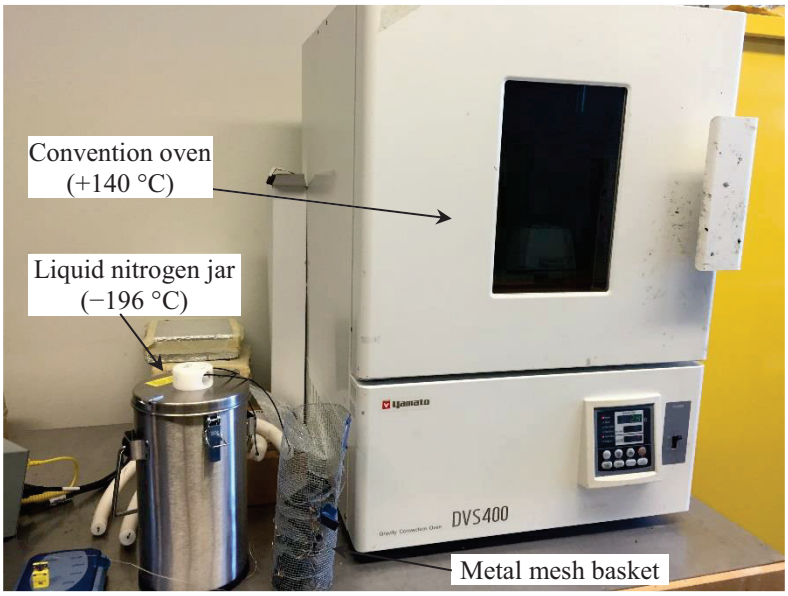

Figure 3-9 Thermal cycling setup including convection oven, liquid nitrogen (LN) container (jar), and metal mesh basket with several shelves to hold samples separate during thermal cycles.

3.5. Material characterization

3.5.1. Thermomechanical Analysis: Coefficient of thermal expansion

The measurements of transverse coefficient of thermal expansion (CTE) were performed using thermomechanical analyzer (TMA), TA instrument Q400. In this machine, sample is placed on the stage of sample holder under an expansion probe with flat tip (Figure 3-10). Machine was operated in standard mode in which the tip applies a constant static load of 0.08 N while the sample is subjected to a linear temperature ramp and simultaneously the sample expansion or contraction is monitored and recorded by the

probe [59]. During the tests, the machine chamber was cooled from room temperature to −70 °C, and then heated to +150 °C and back to room temperature again, with the heating and cooling rate of 5 °C/min. Also, a 10-minute dwell time at either temperature extreme (−70 °C and +150 °C) was done to allow thermal equilibrium to be attained. Five test coupons per laminate were used to measure the CTE. The samples were cut from different areas of the plate in 5 x 10 mm dimensions.

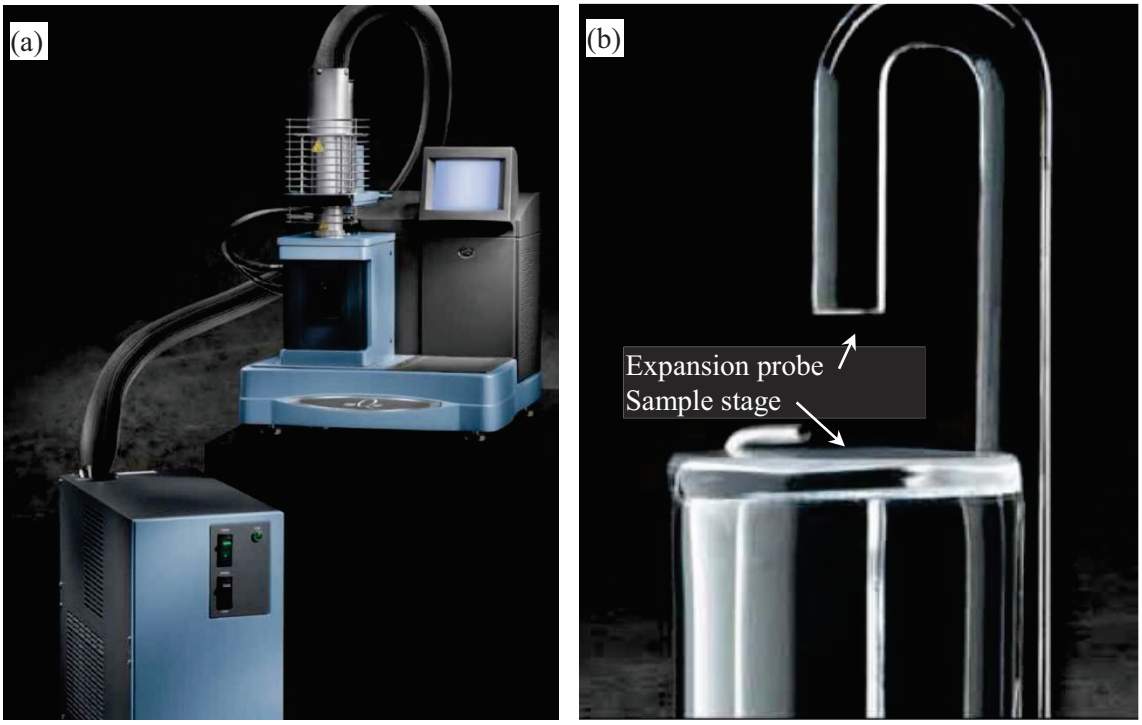

Figure 3-10 (a) TA instrument Q400 Thermomechanical analyzer (TMA); (b) Expansion probe over the sample stage [60].

3.5.2. Dynamic Mechanical Analysis: T_g, storage and loss modulus and damping factor

Dynamic Mechanical Analysis (DMA) provides information about the mechanical properties of a wide variety of materials over a temperature range. DMA can also be utilized to find T_g of the polymer.

Particularly, DMA is used for polymer analysis to study its dynamic moduli. As can be seen in Figure 3-11, when a sinusoidal load is applied to a perfectly solid material (a), the strain would be perfectly in phase with the applied stress. However, for a purely viscos

material (b), a phase lag of 90° would be between stress and resulting strain. Many materials, such as polymers, exhibit both elastic and viscous behavior (c), so they are called viscoelastic materials.

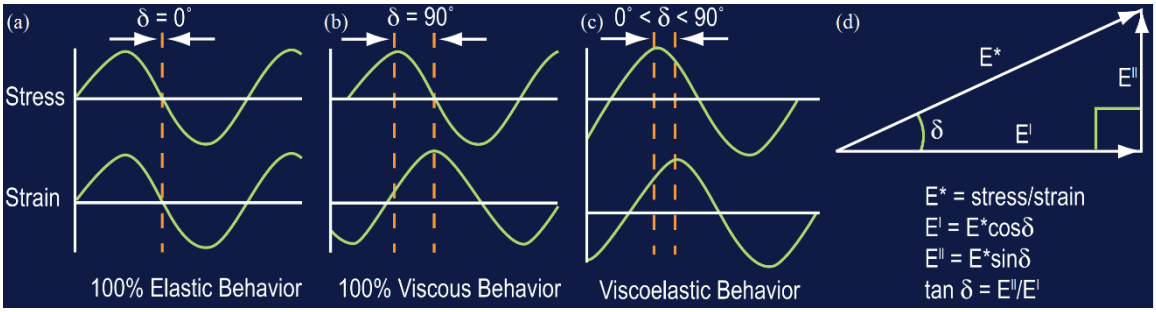

Figure 3-11 Stress-strain behavior of a (a) perfectly elastic, (b) purely viscous, and (c) viscoelastic material. (d) Mathematical relation of complex modulus with storage modulus, loss modulus, and phase difference [61].

Using DMA, one can obtain the complex modulus $E^* = E' + iE''$ in which E', E'', and δ are storage modulus, loss modulus, and phase difference, respectively, and i is the imaginary unit ($i^2 = -1$). The storage modulus is the stiffness of a viscoelastic material and represents the stored energy in a material during a loading cycle. This property is related to the load bearing capacity of the material, such as flexural modulus. The loss modulus E'' represents the viscous component indicating the mechanical energy dissipated through molecular motion from the material during a single loading cycle. Tan δ, the tangent of the phase difference, is actually the loss to storage modulus ratio and is a dimensionless number indicating the energy lost or mechanical damping in a single loading cycle [61], [62]. Complex modulus E^* is equal to strain to stress ratio; knowing E^* and δ, one can easily find the storage modulus and loss modulus from Figure 3-11(d). DMA machines are capable of measuring all these properties as a function of temperature, frequency, and time, for different applications.

There are two important features that make DMA different from other typical tensile testing machines: (i) typical tensile testing machines focus on the elastic behavior of the material while DMA focuses on both elastic and inelastic behavior of the material; (ii) On

the other hand, DMA is more sensitive to structure as it performs in the linear viscoelastic region while typical tensile testing machine performs outside that linear region.

In this project, dynamic mechanical analyses were conducted using a TA instrument Q800 (Figure 3-12). The specimens with dimensions of 50 mm × 15 mm ×3 mm were used for the analysis. The analyses were done in three-point bending mode in which a force is applied to the middle of the sample along its length while both ends are clamped. The force was applied at a frequency of 1 Hz. The advantage of three-point bending fixture is that the clamping effect is eliminated and there is pure deformation using low-friction roller bearings with a clamp span of 50 mm. In order to operate the test at sub-ambient temperatures, a Gas Cooling Accessory (GCA) was connected to the DMA to cool the chamber using cold nitrogen gas [61]. The samples were heated from −150 °C to +320 °C at a heating rate of 5 °C/min with a maximum displacement of 0.05 mm at the middle of span length.

T_g can also be found from DMA analysis. T_g is a temperature above which the polymer behavior changes from glassy to rubbery with significant drop in stiffness and enhance in viscosity. Thus, storage modulus decreases while loss modulus increases which means that tan δ increases dramatically [63]. Hence, the glass transition temperature was determined from the peak of the tan δ curve.

Tests were conducted for each laminate with a minimum of two similar samples.

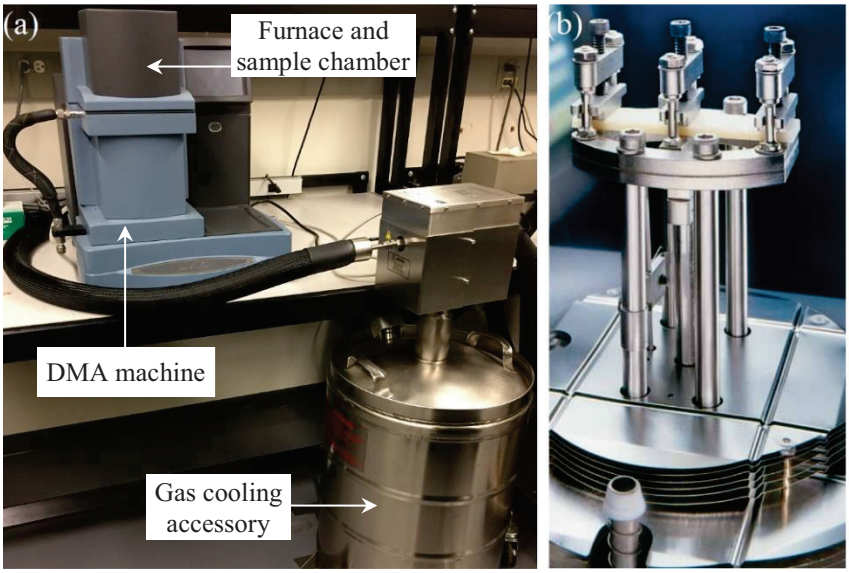

Figure 3-12 (a) TA instrument Q800 DMA machine connected to gas cooling accessory, (b) Three point bending fixture [64].

3.5.3. Short Beam Shear Test: Interlaminar shear strength

The interlaminar shear strength (ILSS) theory was briefly explained in previous chapter, section 0. In this research, ILSS tests were conducted in accordance with ASTM-D 2344-13 standard test method for three-point bending at 22 °C and 50% relative humidity. To perform the test, MTS 810 machine (a servohydraulic testing systems) was utilized together with Wyoming three-point test fixture. Figure 3-13 depicts the MTS machine with the fixture for three-point bending test as well as a specimen under test. Test was run at a crosshead speed of 1 mm/min on a support span of 14 mm in accordance with ASTM D344-13 standard test method. The width and thickness of all specimens were measured three times and the average value was used for calculations.

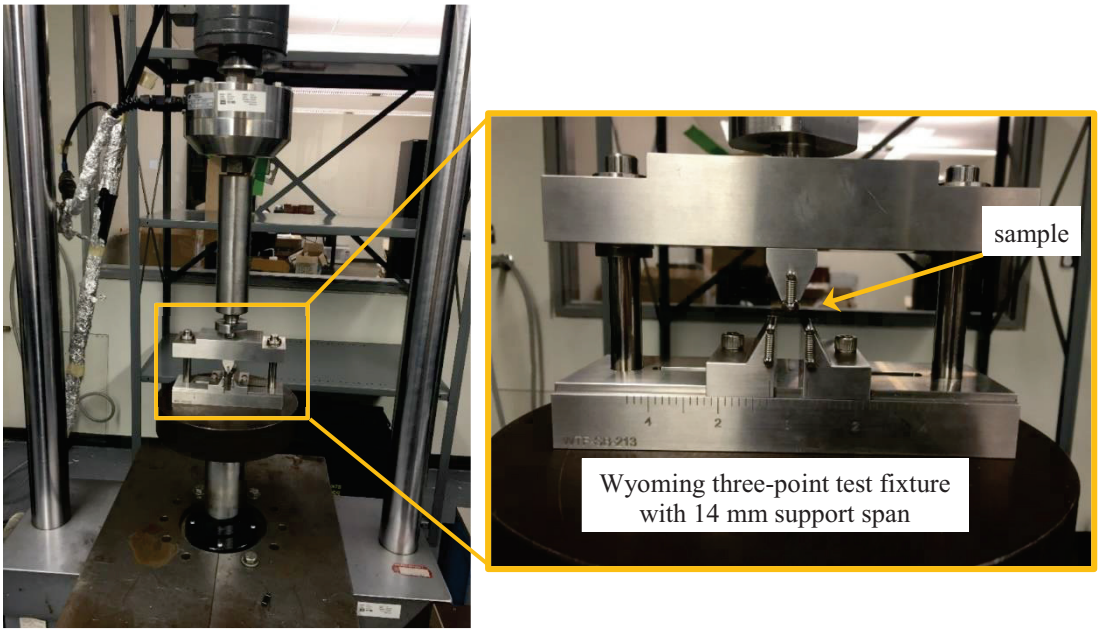

Figure 3-13 MTS 810 testing machine with a Wyoming three-point bending test fixture for interlaminar shear strength testing

3.5.4. Total number of samples and tests

According to the experimental plan, in total, 153 specimens were tested for conducting this research as below:

- 88 UD specimens, including 80 for ILSS testing, 5 for CTE testing, 2 for DMA, and 1 for microscopy;
- 63 fabric specimens, including 55 for ILSS testing, 5 for CTE, and 2 for DMA, and 1 for microscopy;
- and two specimens from sandwich panel for microscopy.

It should be noted that the non-destructive testing including CTE and DMA were performed on the same specimens after reaching each thermal cycle target, *i.e.*, 0, 30, 60, 100, 150 and 200 cycles. The optical microscopy images were taken even more often. Therefore, the total number of testing was 241 including:

- 143 ILSS tests,
- 60 CTE tests,
- 30 DMA tests,
- and 55 microscopy.

Chapter 4: Results and Discussion

In this chapter, the experimental results are presented followed by a comprehensive discussion. In the first three parts of the chapter, results of unidirectional (UD) laminate, cross-ply fabric laminate made of 5HS fabric (hereinafter referred to as cross-ply fabric for ease of reference), and sandwich panel is presented. The stacking sequence for UD and fabric laminate is $[0]_{24}$ and $[(0/90)/ (0/90)]_{2s}$ respectively.

For UD and fabric laminates, the results of the degree of cure, microscopy, ILSS test, dynamic mechanical analysis (including loss and storage modulus, tan δ, and T_g), and coefficient of thermal expansion is presented. For the sandwich panel, only the microscopy observation was done and is reported. In the last part of the chapter, the results will be quantitatively and qualitatively discussed in detail.

4.1. Unidirectional laminate

In this section, unidirectional flat laminate made of unidirectional tape prepreg ($[0]_{24}$) manufactured OOA is examined.

4.1.1. Degree of cure

DSC test was performed on the UD composite plate to obtain the degree of cure. Five samples were cut from different areas of the UD plate in order to have an average

representative of the whole plate. Figure 4-1 shows the DSC heat flow signal for both uncured prepreg and cured laminate as a function of temperature. A linear integration of the area under the heat flow curve was used to calculate the total heat of reaction for both uncured and cured materials which resulted in 176.6 J/g for the raw prepreg and 10.54 J/g for the cured laminate. Based on the data obtained from DSC graphs, the average degree of cure for the UD laminate was 94.03% which indicate a good curing process. It should be mentioned that the degree of cure for the plate was calculated as the average value of five different samples per category.

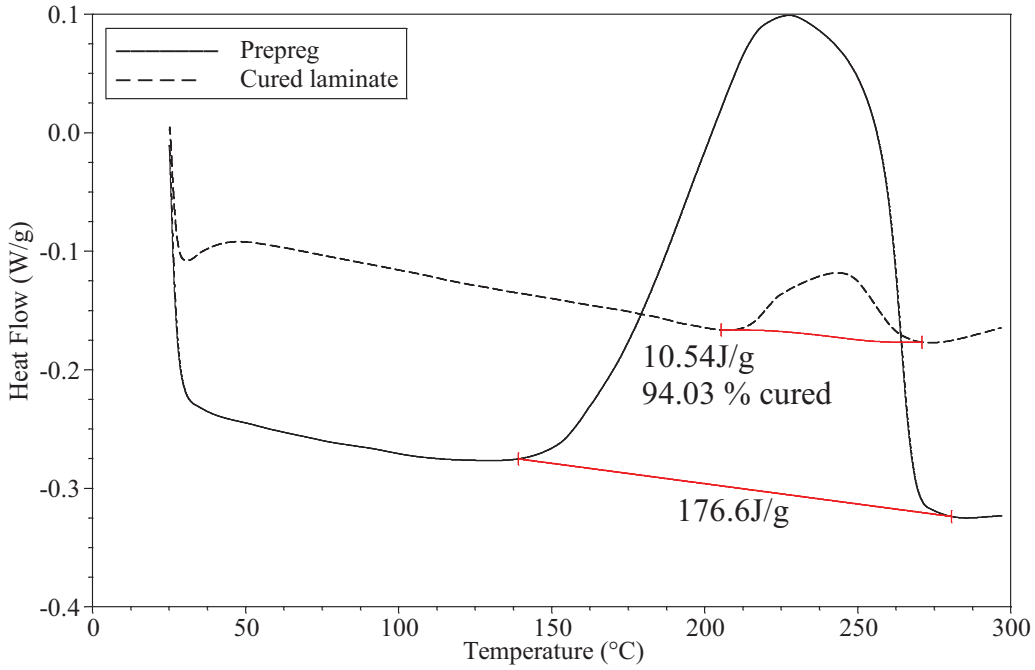

Figure 4-1 Heat flow of uncured prepreg and cured laminate for UD composite obtained from DSC

4.1.2. Microcrack observation

Optical microscope was utilized to observe the response of the composite samples to thermal cycling in terms of crack initiation and propagation. Polished UD samples were observed at 20X magnification prior to cycling to make sure that there is no microcrack in the surface; however, there were some voids in the samples due to the OOA curing of the material and absence of oven pressure during the cure. Samples were taken for microscopy after 1, 5, 10, 20, 50, 100, 150, 200, 250, 300, and 350 cycles. As can be seen in Figure 4-2, microcracks appeared after 350 thermal cycles. Cracks started to form by

connecting the adjacent voids together and causing delamination cracks between the layers (left inset). A few cracks were also formed within a single ply due to linking of the voids. All the cracks observed were horizontal and no vertical crack was found through the entire laminate.

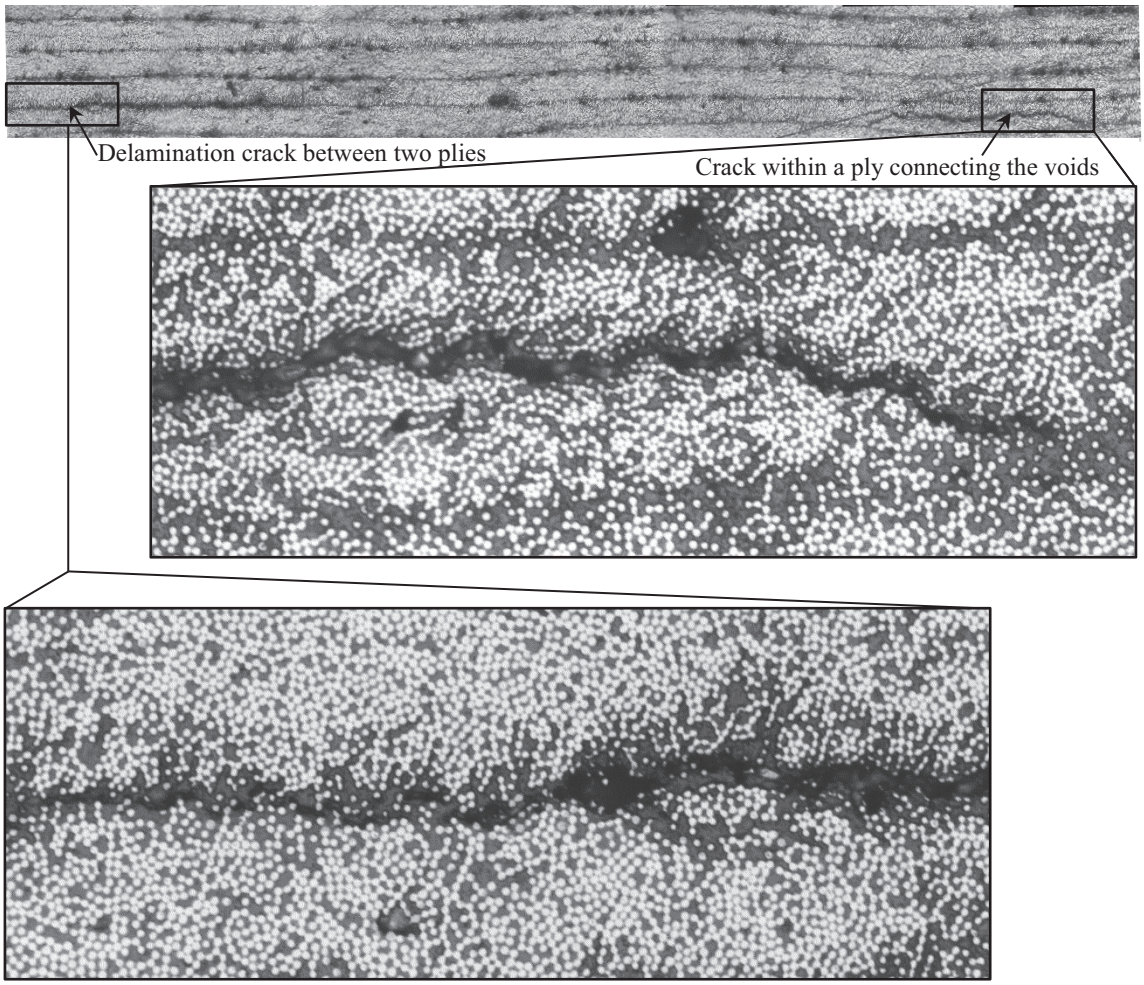

Figure 4-2 Optical microscope image of UD laminate. Adjacent voids were connected to form horizontal microcracks within a single ply (right inset) and also between two plies (left inset) to delaminate the composite.

4.1.3. Interlaminar Shear Strength (ILSS)

To evaluate the shear strength of matrix layers between adjacent plies, the interlaminar shear strength (ILSS) test was conducted on UD laminate composites. A typical force-displacement curve for a UD laminate sample before being exposed to thermal cycling is

displayed in Figure 4-3. The specimen broke at maximum load of 2789 N followed by a sharp load drop due to interlaminar shear failure. Using Equation (1), the $ILSS_{UD}$ = 99.21 MPa. The specimen before and after ILSS test along with the accepted modes of failure is shown in Figure 4-4. As can be seen, the actual failure shown in Figure 4-4(b) is an accepted failure mode according to ASTM D2344.

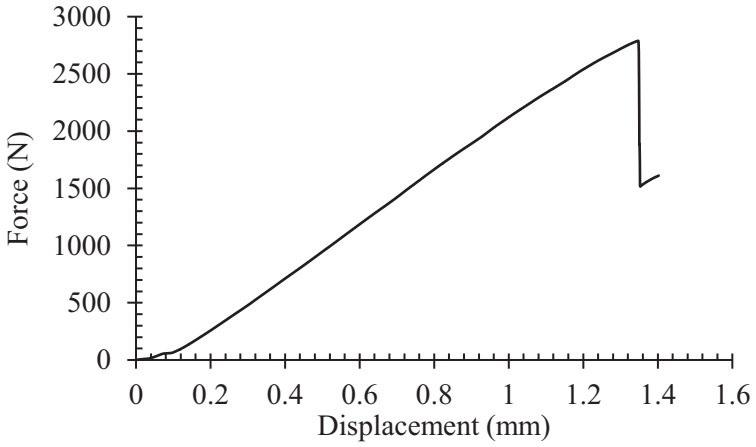

Figure 4-3 Force-displacement curve of interlaminar shear test of a unidirectional laminate composite unexposed to thermal cycling.

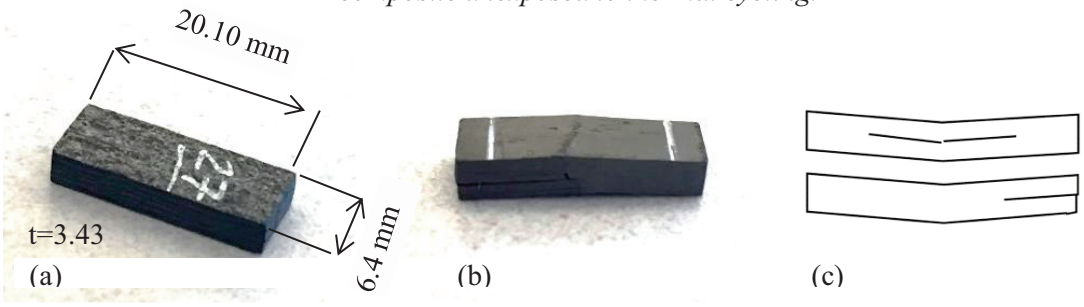

Figure 4-4 A unidirectional specimen in three-point bending test (a) before test, (b) and after test. (c) Two accepted modes of interlaminar shear failure from standard ASTM D2344

Figure 4-5 shows the variation of the ILSS of the present carbon/epoxy composite versus different thermal cycles for UD plate. The values documented are the average of 5 specimens. For a better comparison, Table 4-1 lists the change rate and coefficient of variation (CV) of the ILSS results of UD samples. The ILSS of the UD composite first gradually decreased until 100 cycles by 8.32% from 99.21 MPa for unexposed sample to 90.96 MPa. Afterward, it increased about 11.27% with further cycling to 101.21 MPa for 200 cycles, which is about 2% higher than the unexposed one. The same trend was

reported already by Gao *et al.* [47] as shown in shown in Figure 2-4 (d). However, since the CV of the results is of the same order as the changes in the mean values and also the fluctuations are not consistent, it is not easy to conclude a trend.

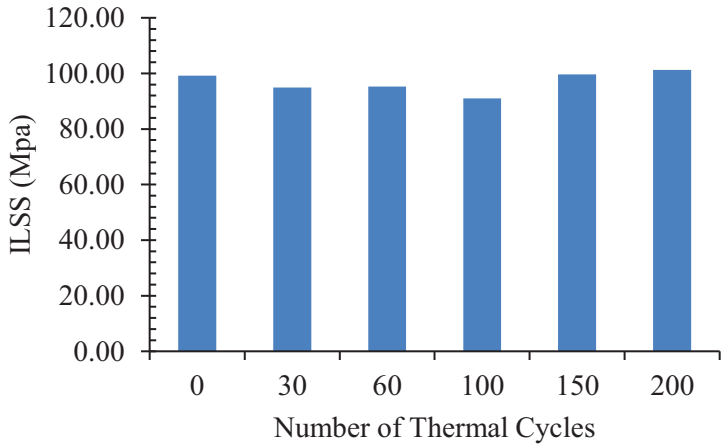

Figure 4-5 Interlaminar shear strength (ILSS) of unidirectional composite subjected to different thermal cycles

Table 4-1 Change rate and coefficient of variation (CV) of ILSS results of unidirectional composite subjected to different thermal cycles

No. of cycles	ILSS (MPa)	CV (%)	Change rate (%) wrt previous cycle	Change rate (%) wrt 0-cycle
0	99.21	6.47	n/a	0
30	94.95	9.74	−4.29	−4.29
60	95.26	6.17	+0.33	−3.98
100	90.96	4.55	−4.51	−8.32
150	99.66	6.94	+9.56	+0.45
200	101.21	6.54	+1.56	+2.02

4.1.4. Dynamic Mechanical Analysis

Dynamic Mechanical Analysis (DMA) was conducted to examine the variation of storage modulus (E′), loss modulus (E″), tan δ, and T_g of the samples after being exposed to thermal cycling in comparison with unexposed samples. Storage modulus and loss modulus represent the dynamic elastic and dynamic plastic (or viscos) response of the material, respectively, and tan δ is their ratio (tan δ = E″/ E′) [65]. Since the modulus of the carbon fiber is not changing in the temperature range studied in this thesis, the variations of loss and storage modulus represent the variations in polymer and/or

polymer/fiber interface [66]. The reported results of DMA are based on the average value of two specimens.

Figure 4-6 shows the dynamic mechanical properties of UD laminate before being exposed to thermal cycling. The storage modulus, loss modulus and damping factor (tan δ) during exposure to extreme temperatures from −150 ˚C to +320 ˚C are shown. As can be seen in this figure, storage modulus (E′) of the laminate decreased with increasing the temperature, indicating that the laminate became less elastic by increasing the temperature. In the temperature range of −150 °C to +160 °C, E′ gradually decreased by about 34% which means that the material was still in its glassy region. A sharp decline in E′ can be seen from +160 °C to +235 °C where the material transition from glassy to rubbery state happened. Finally, with increasing temperature from +235 °C, E′ values tends to very low values which indicates material was in rubbery state and the moduli above +235 °C degraded. With increasing the temperature, loss modulus value and Tan δ value increased and attained a peak value which again decrease with the increase in temperature.

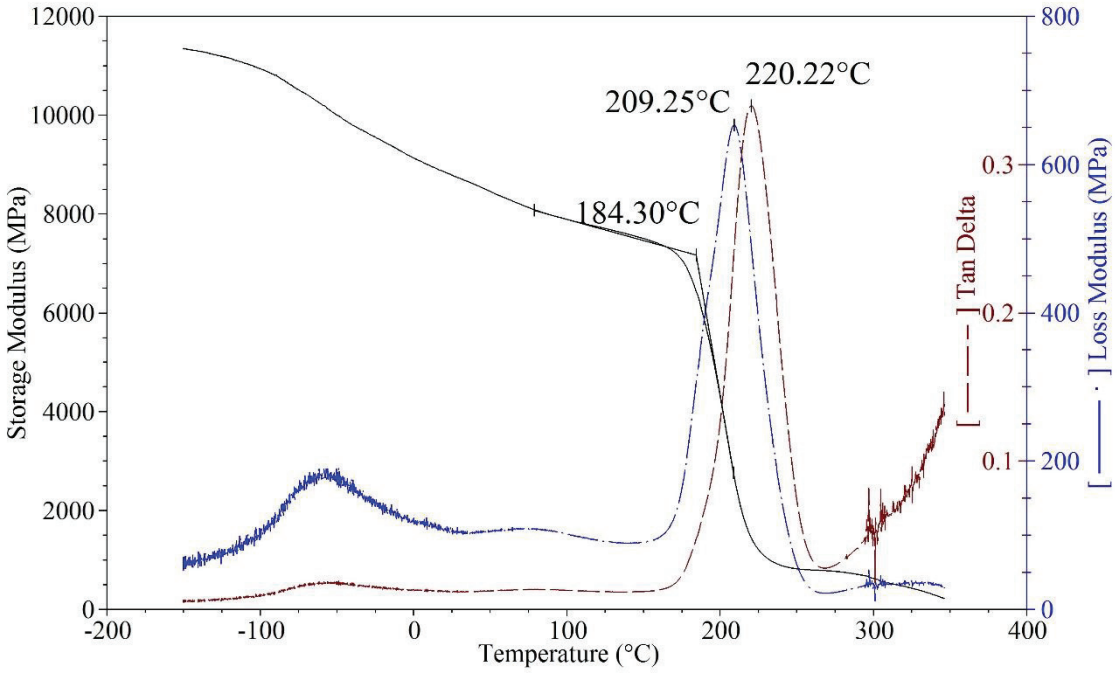

Figure 4-6 Dynamic mechanical response of unidirectional laminate in 90° vs temperature before being exposed to thermal cycling.

Thermal cycling effect on Storage Modulus

Figure 4-7 shows the effect of thermal cycling up to 350 thermal cycles on the storage modulus of the UD composite in 90° direction. As the number of thermal cycles increases, storage modulus decreases with the same trend despite some minor fluctuations in between. To be more accurate, the storage modulus at three different temperatures of −150 °C, +25 °C, and +220 °C is shown for comparison in Figure 4-8. The high temperature was selected as 220 °C which is around T_g. As a result of exposure to thermal cycles, by the increase in the number of thermal cycles up to 350 cycles, the storage modulus of the UD composites decreases at extreme low (−150 °C) and room (+25 °C) temperature by about 8% and 3%, respectively. At high temperature close to the T_g, the decreases in the storage modulus is about 43% after 350 cycles. Since the material at this high temperature is practically a viscose material with very small storage modulus $E' = 1415$ MPa compared with room temperature ($E'_{+220°C} < 0.16\ E'_{+25°C}$), there is no point to further discuss on the storage modulus at very high temperature.

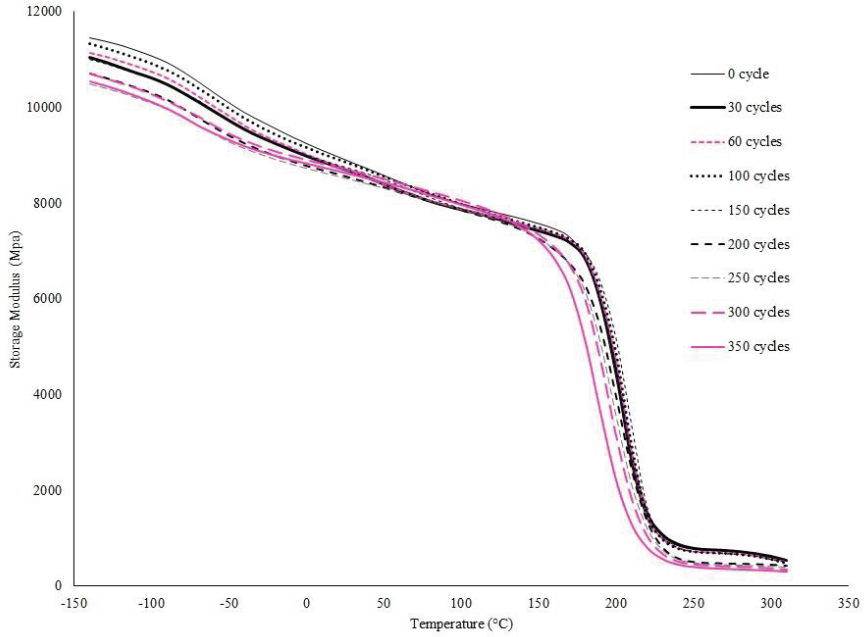

Figure 4-7 Effect of thermal cycling on storage modulus of unidirectional composites in 90° direction.

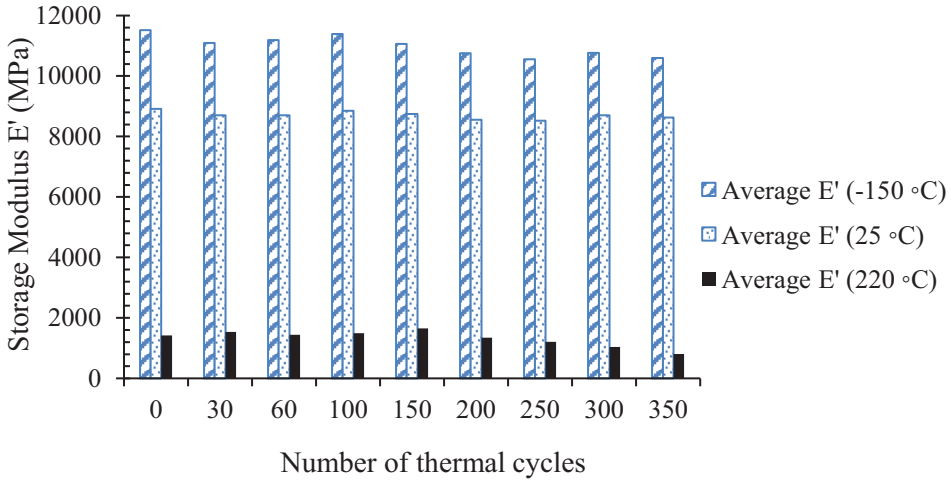

Figure 4-8 Variation of storage modulus in matrix direction of unidirectional compsoite vs the number of thermal cycles at low (−150 °C), room (+25 °C), and high (+220 °C) temperature.

Thermal cycling effect on Loss Modulus

The effect of thermal cycling on loss modulus was also studied by DMA test and the results are exhibited in Figure 4-89. Loss modulus represents the mechanical energy dissipation through molecular motion and its peak is related to molecular friction above the glass transition temperature. The peak value was measured after different number of thermal cycles. By increasing the number of thermal cycles up to 150 cycles, the loss modulus peak value had some fluctuation of less than 2.2% within $E''_{unexposed}$ = 658 MPa. After 150 thermal cycles, the loss modulus increased continuously by the increase of cycles and reached to $E''_{350\text{-}cycle}$ = 751 MPa which is about 14% higher than unexposed sample.

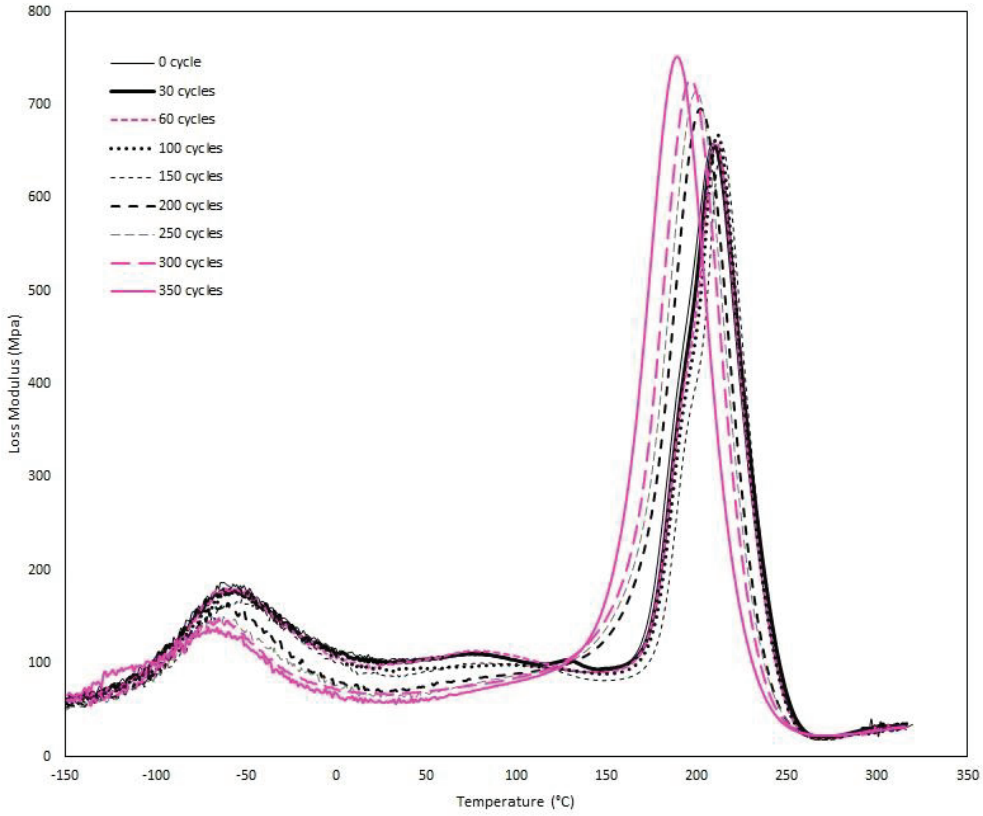

Figure 4-9 Effect of thermal cycling on the loss modulus of UD composites in 90° direction.

Thermal cycling effect on Tan δ

Tan δ is the ratio of loss to storage modulus. Figure 4-10 shows the variation of tan δ of the UD laminate subjected to different thermal cycles. For the first 150 thermal cycles, tan δ exhibited some fluctuation of less than 6% with respect to the unexposed samples. Then, by increasing the number of thermal cycles from 150 to 200 cycles it suddenly decreased by ~19% and stayed almost constant with further cycling to 350.

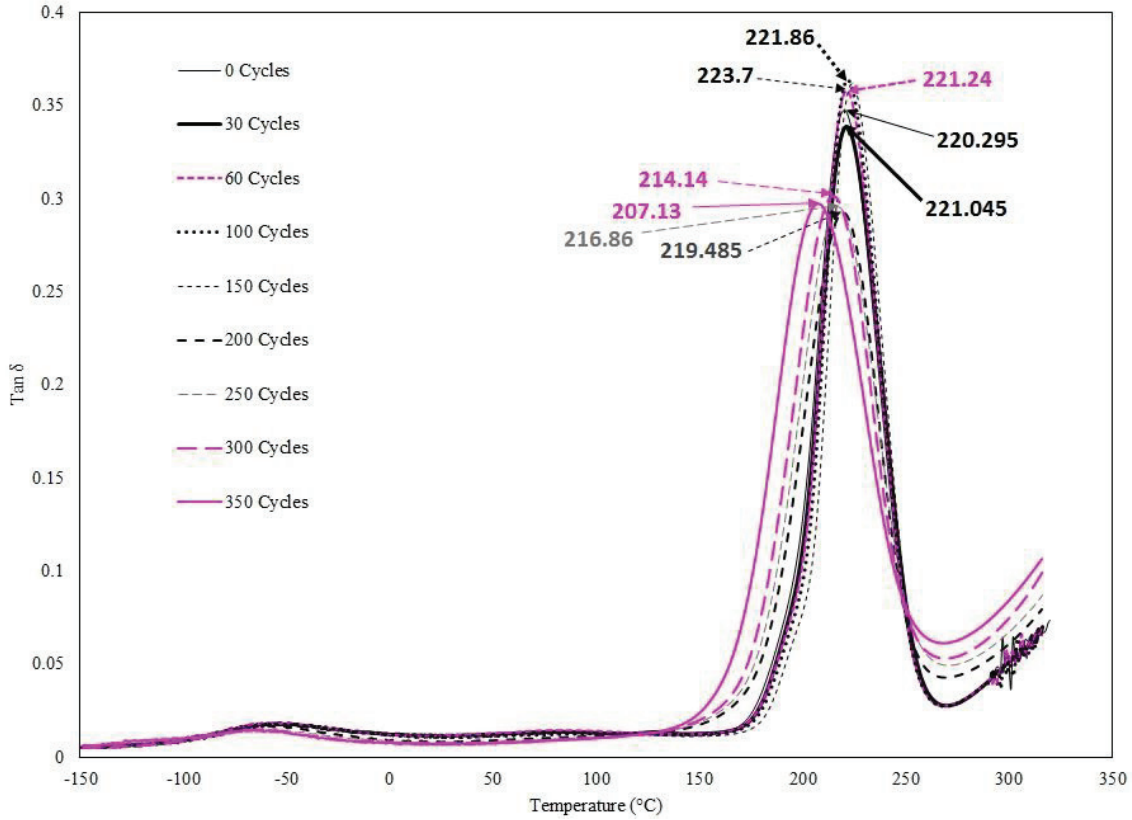

Figure 4-10 Effect of thermal cycling on tan δ of UD composites in 90° direction.

Thermal cycling effect on T_g

Glass transition temperature T_g can be found from the curves of storage modulus, loss modulus, and tan δ vs temperature in a DMA analysis; however, it is often preferred and more accurate to locate T_g from the peak of tan δ. The value of T_g is marked in peak of tan δ in Figure 4-10; for a better comparison, the variation of T_g vs. cycles is shown in Figure 4-11. At the beginning of thermal cycles T_g of UD composite samples tends to continuously rise by 1.6% from 220.3 °C of unexposed sample to 223.7 °C at 150 cycles. Then it decreases by 7.4% with further cycling to 207.1 °C at 350 cycles which is about 6% lower than T_g of unexposed sample. This trend indicates that during the thermal cycling, the rising temperature can cause more degree of crosslinking of the resin matrix which consequently induces post curing to some extent. Further cross linking causes increase of T_g. However, this trend disappears after 150 cycles as reported by other researchers [7], [11], [47].

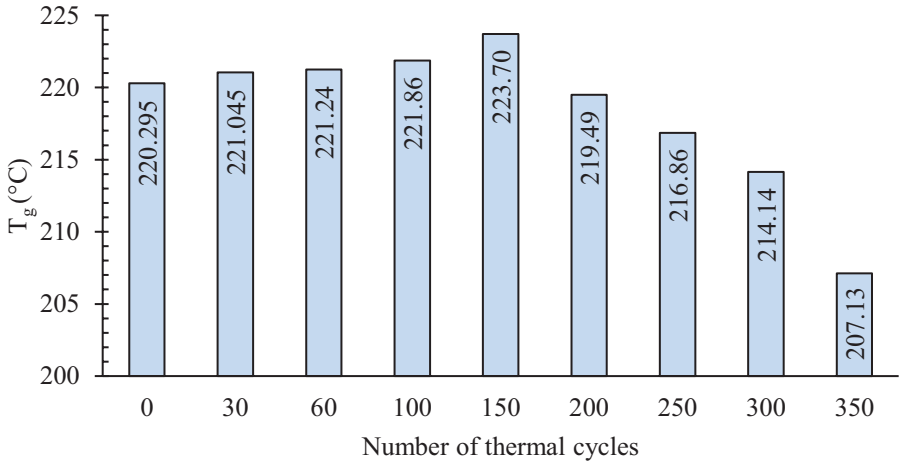

Figure 4-11 Variation of T_g of unidirectional laminate vs. the number of thermal cycles.

4.1.5. Linear Coefficient of Thermal Expansion

TMA tests were conducted to measure the transverse coefficient of thermal expansion (CTE) (or called CTE through-the-thickness) over a temperature range of −70 °C to +150 °C. Figure 4-12 shows the CTE variation of UD composite with the number of thermal cycles. For a better comparison of the results, a polynomial trend line is used to fit to the curve as shown in the inset figure. CTE of UD composite, even though exhibits fluctuations, first jumps to a higher value when exposed to 60 cycles. By increase of cycles to 100, CTE decreases for smaller amount compared with its initial jump. Further cycling up to 200 cycles indicates no significant change in the CTE of the unidirectional composite samples. Thus, thermal cycling, all in all, caused an increase in through-the-thickness CTE of UD composite compared with unexposed samples.

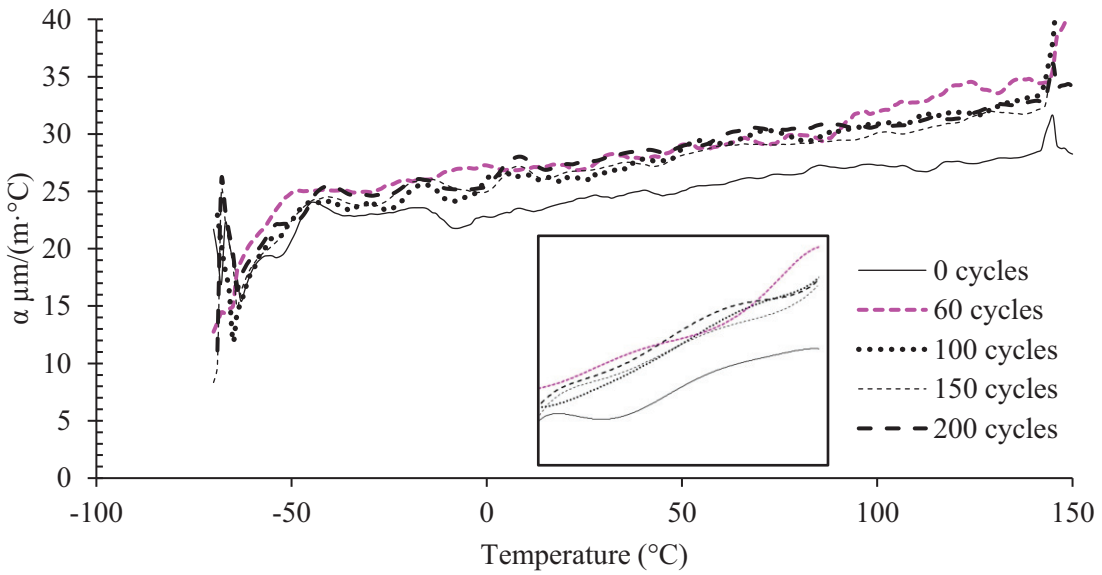

Figure 4-12 Effect of thermal cycling on through-the-thickness CTE of unidirectional composites. The inset presents polynomial trend lines fitted to CTE curves.

4.2. Cross-ply fabric laminate

In this section, cross-ply laminate made of 5HS fabric prepreg with the stacking sequence of $([(0/90)/ (0/90)]_{2s}$ is examined.

4.2.1. Degree of cure

DSC tests on cross-ply fabric were performed following the same procedure as the one used for UD samples to find out the cure degree. The heat flow signal as a function of temperature for both uncured prepreg and cured laminate are shown in Figure 4-13. Based on the data obtained from DSC graphs, the average degree of cure for the cross ply fabric laminate is 98.00%.

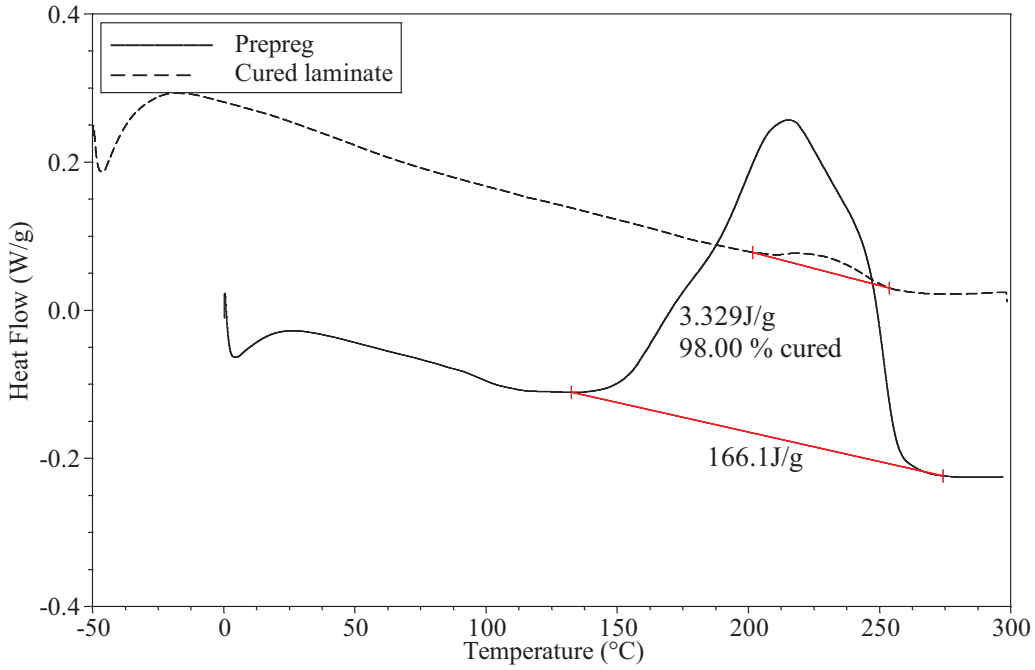

Figure 4-13 Heat flow of uncured prepreg and cured laminate for cross-play fabric laminate obtained from DSC

4.2.2. Microcrack Observation

Samples of cross-ply fabric laminate were observed at 20x magnification in search for microcracks and voids. Microscopy was first done prior to cycling to make sure that there is no microcrack in the surface. The same as UD, there were several voids as expected due to OOA manufacturing. Samples were taken for microscopy after 1, 2, 3, 4, 5, 10, 20, 30 and 40 thermal cycles. The results of microscopy are shown in Figure 4-14 for the first five cycles and Figure 4-15 for cycles 10 to 40. Unlike UD samples that there was no crack up to 350 thermal cycles, imaging of cross-ply specimen demonstrates the presence of several microcracks in early cycles. Several cracks were detected at edges and also around the voids; *e.g.* figure (c) demonstrate that after one cycle a crack was initiated at the upper edge of laminate and propagated until reached the 0° fiber. However, on the left side of the section around the specified void, there was no crack up to 4 cycles and then a crack was initiated around the void after the fifth cycle. All the detected cracks started to grow in 90° plies; by the increase of thermal cycles cracks propagated through the whole thickness of the ply and stopped when reaching 0° plies.

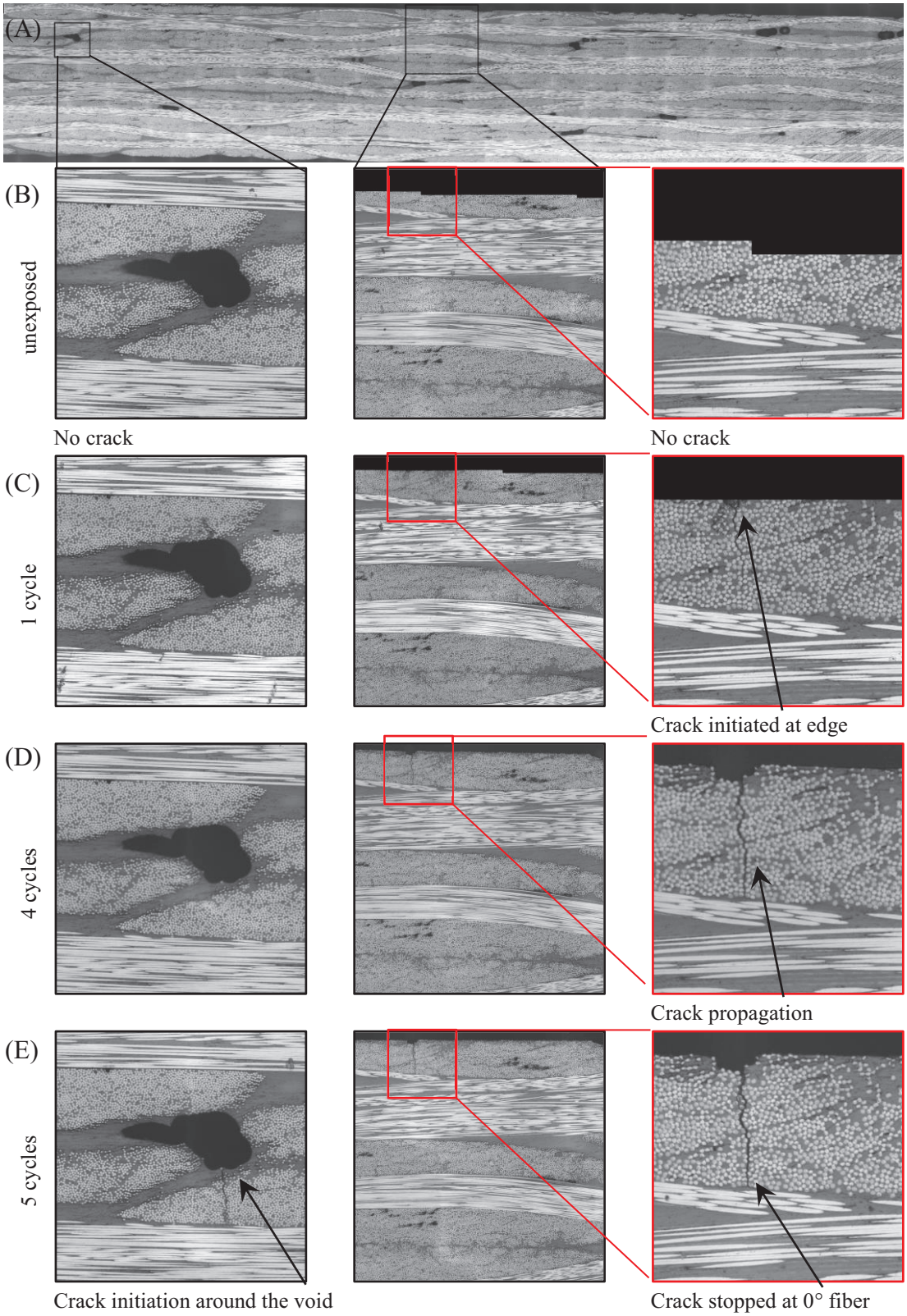

Figure 4-14 Optical microscope image of cross-ply fabric laminate; (a) before exposure to thermal cycle; after (b) 1 cycles; (c) 4 cycles; (d) 5 cycles. Cracks imitation and propagation around the void and close to edge are demonstrated.

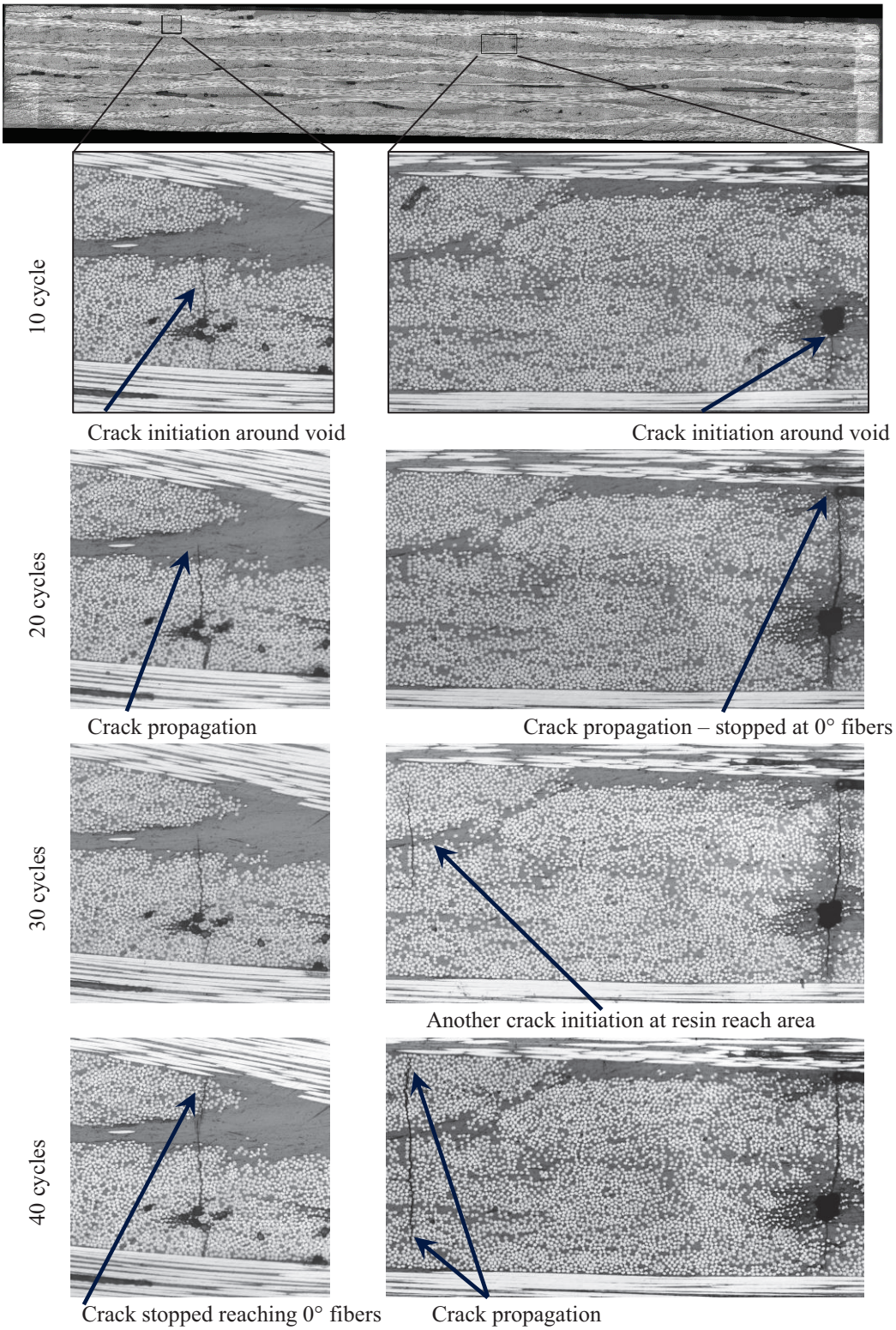

Figure 4-15 (a) Optical microscope image of cross-ply fabric laminate after several thermal cycles: (a) 10 cycles; (b) 20 cycles; (c) 30 cycles; (d) 40 cycles. Cracks imitation and propagation around the void and at resin reach areas are demonstrated.

4.2.3. Interlaminar Shear Test:

Figure 4-16 shows a typical force-displacement curve obtained from three-point bending test of cross-ply fabric sample before exposure to thermal cycles. The maximum load that specimen carried was 1711 N and then the load dropped due to interlaminar shear failure at midplane. Using Equation (1), the ILSS $_{\text{cross-ply}}$ = 63.39 MPa which is about 36% less than ILSS of UD laminate.

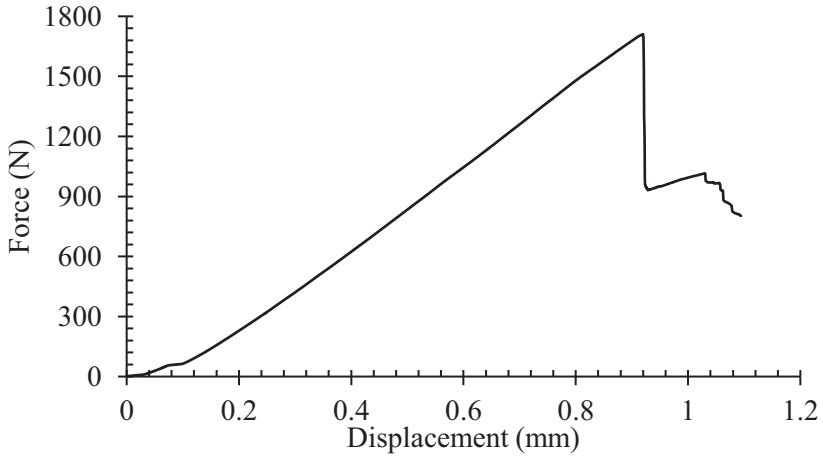

Figure 4-16 Force-displacement curve of interlaminar shear test of a cross-ply fabric laminate unexposed to thermal cycling.

Figure 4-17 shows the variation of the ILSS of the present cross-ply fabric laminate versus different number of thermal cycles. As can be seen in this figure, with increasing the number of thermal cycles from 0 to 200, the ILSS of the composites gradually decreased by 9.6% from 63.39 MPa for unexposed sample to 57.31 MPa for 200 cycles. The change rate and coefficient of variation (CV) of the ILSS results of cross-ply fabric laminate samples are listed in Table 4-2. Since the change rate of mean values from one cycle set to the next one are in the same range of the CV of the results, the conclusion for ILSS degradation vs. number of thermal cycles is not a firm conclusion.

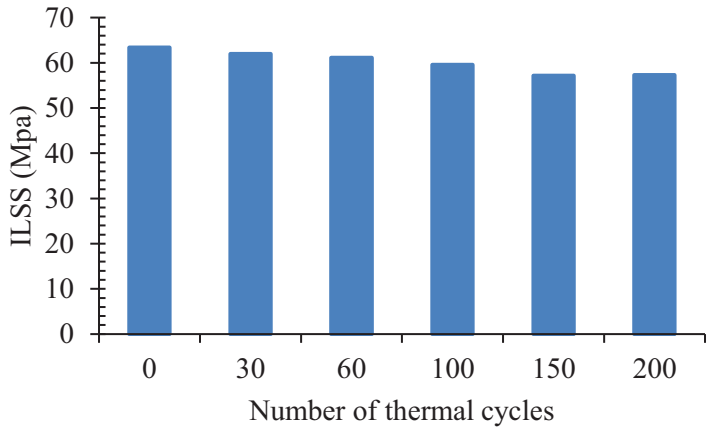

Figure 4-17 Interlaminar shear strength (ILSS) of cross-ply fabric laminate subjected to different thermal cycles

Table 4-2 Change rate and coefficient of variation (CV) of ILSS results of cross-ply fabric laminate subjected to different thermal cycles

No. of cycles	ILSS (MPa)	CV (%)	Change rate (%) wrt previous cycle	Change rate (%) wrt 0-cycle
0	63.39	4.15	n/a	0
30	61.98	2.88	-2.22	-2.22
60	61.14	3.06	- 1.36	-3.55
100	59.57	2.94	- 2.57	-6.03
150	57.16	2.99	- 4.05	-9.83
200	57.31	4.52	+0.26	-9.59

4.2.4. Dynamic Mechanical Analysis

DMA test was conducted to examine the effect of thermal cycling on storage modulus (E′), loss modulus (E″), tan δ, and T_g of the samples. The reported values are the average of two specimens.

Figure 4-18 shows the DMA results of cross-ply fabric laminate before exposure to thermal cycling. The storage modulus, loss modulus and damping factor (tan δ) as a function of temperature from −150 ˚C to +320 ˚C are shown. Unlike the UD laminate whose E′ continuously decreased with temperature, E′ of fabric laminate at low temperatures showed a decrease of about 9% from 52.1 GPA at −150 °C to 46.9 GPa at room temperature and then a slight increase of 2% to 48.2 GPa at +183 °C. This behavior which happened well below T_g is expected for traditional woven glassy composites as

reported by Wrublewski [67]. Loss modulus after this temperature experienced a sharp drop indicating that the polymer became rubbery and the moduli above +275 °C degraded. The same as UD, loss modulus and tan δ increased with temperature increase and attained a peak value after which decreased with the increase in temperature.

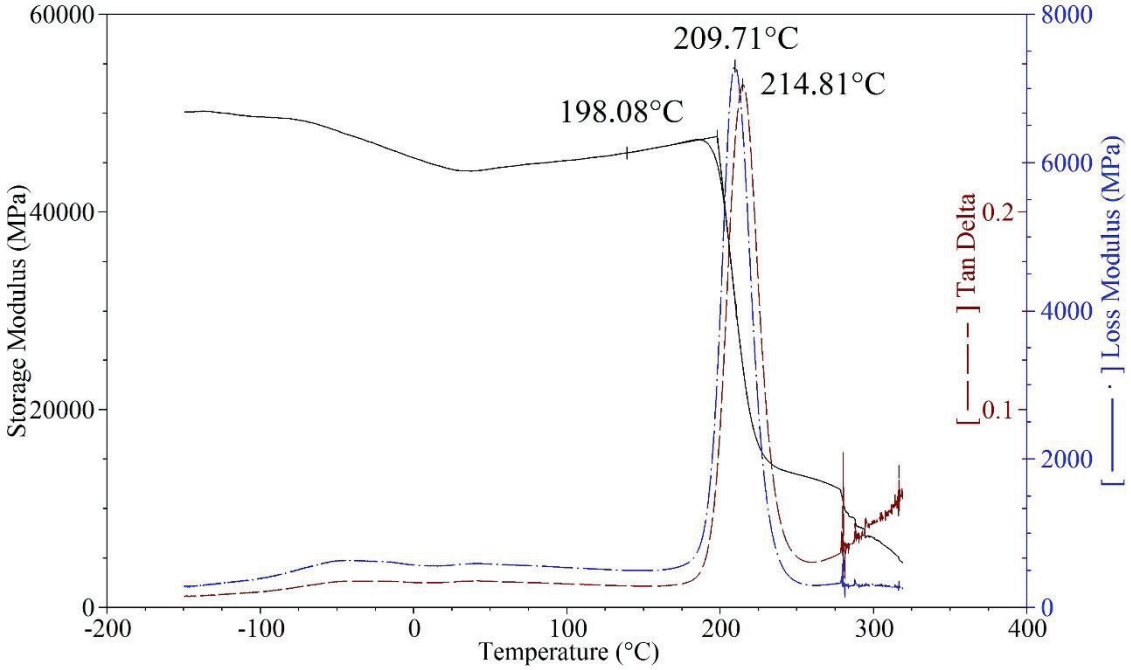

Figure 4-18 Dynamic mechanical response of unidirectional laminate vs temperature before being exposed to thermal cycling.

Thermal cycling effect on Storage Modulus

Figure 4-19 shows the variation of storage modulus E′ of the cross-ply composite as a result of thermal cycling. The storage modulus tends to significantly decrease as the number of thermal cycles increase. At extreme low temperature of −150 °C, storage modulus reduces from 52.1 GPa for unexposed sample to 39.1 GPa for 200 times cycled sample which is equivalent to 25% reduction in storage modulus as a result of thermal cycling. This reduction for room temperature is about 19% from $E'_{unexposed}$ = 44.3 GPa to $E'_{200\text{-}cycles}$ = 36.0 GPa.

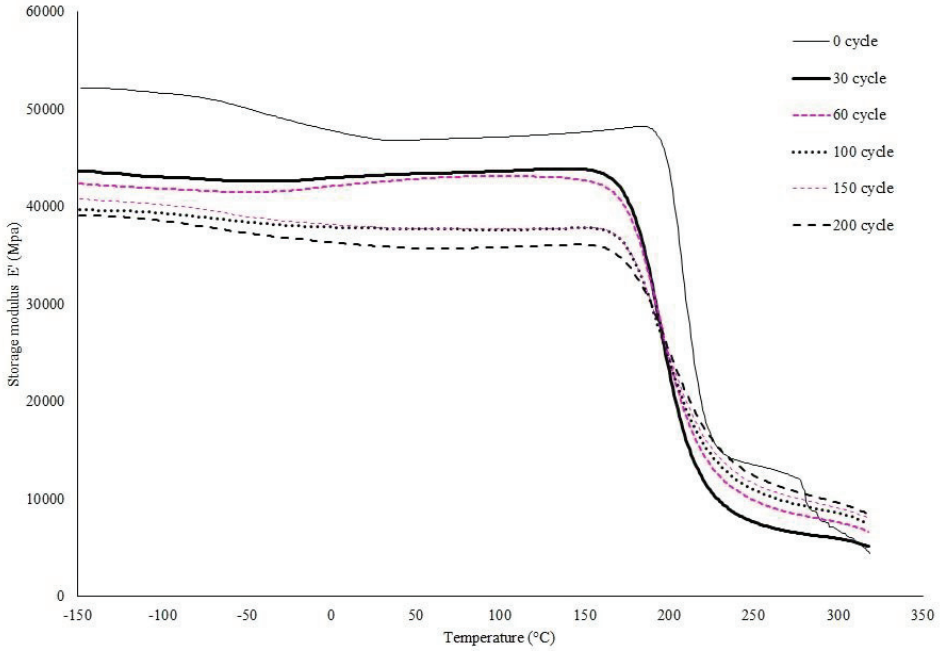

Figure 4-19 Effect of thermal cycling on storage modulus of cross-ply fabric laminate in 90° direction.

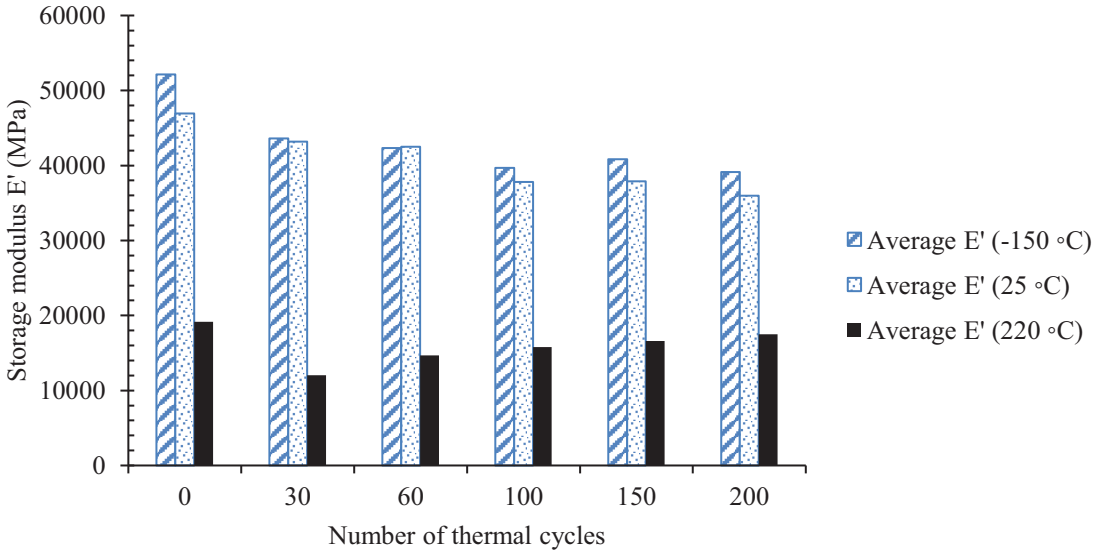

Figure 4-20 Variation of storage modulus in 90° direction of fabric composite vs the number of thermal cycles at low (−150 °C), room (+25 °C), and high (+300 °C) temperature.

Thermal cycling effect on Loss Modulus

Figure 4-20 exhibits the thermal cycling effect on the loss modulus (E″). It can be found from the peak of loss modulus that it fell significantly by increasing the number of thermal cycles. The reduction rate is very significant at early cycles such that $E''_{30\text{-cycles}}$ = 5.13 GPa which is about 30% less than $E''_{unexposed}$ = 7.32 GPa. This reduction rate slows down by further cycling up to 200 cycles where $E''_{200\text{-cycles}}$ = 3.23 GPa which is about 56% less than unexposed. It is clear from the figure that with increase of thermal cycles, the magnitude of the peaks decreases while the curve at peak area gets broader (unlike UD).

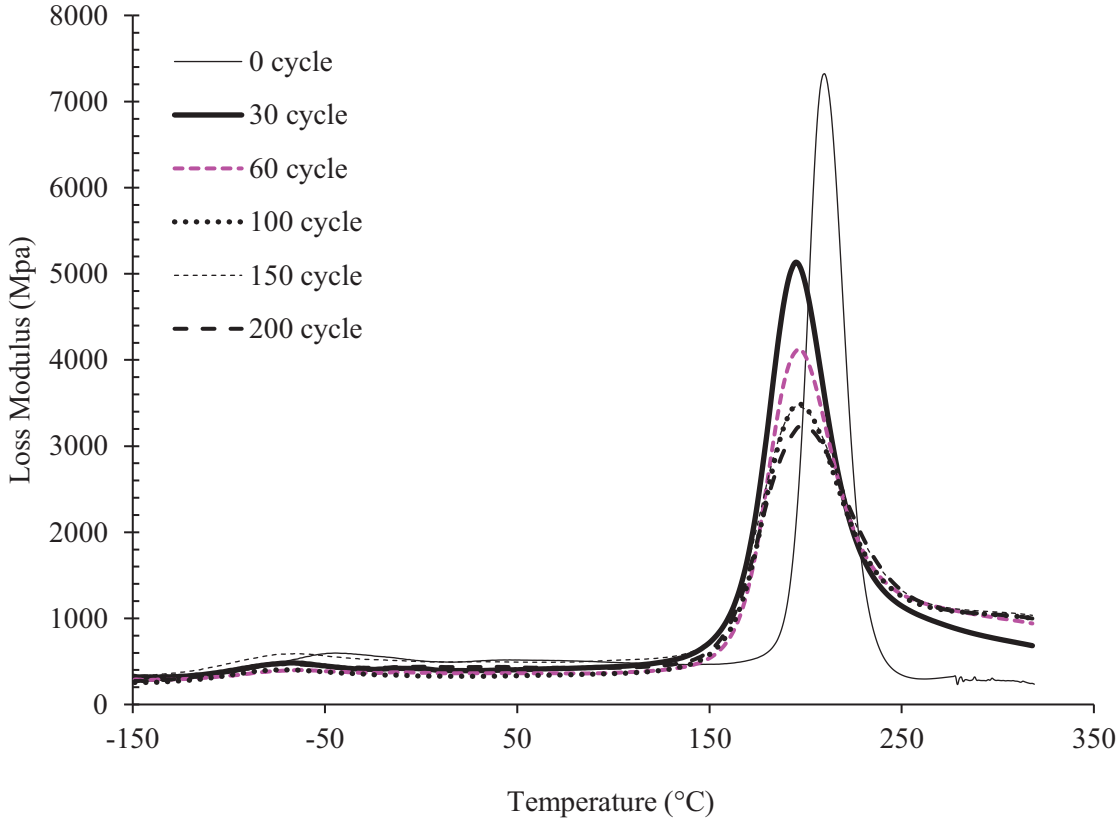

Figure 4-20 Effect of thermal cycling on the loss modulus of cross-ply fabric laminate in 90° direction.

Thermal cycling effect on Tan δ

Figure 4-21 shows the thermal cycling effect on the tan δ of cross-ply fabric laminate in 90° direction. It can be seen that the peak of tan δ decreases continuously by increasing the number of thermal cycles but the reduction rate is not the same for all cycles. For the first

100 cycles, tan δ drops by an average rate of 16% and afterward it slows down. The reduction of tan δ was 46% from 0 to 200 thermal cycles. It is clear from the curves that by increase of thermal cycles, the peak values decrease while the curve broaden. The same behavior was observed for UD laminates but not as evident as cross-ply fabric laminate. This indicates that stiffness increased while viscosity decreased which probably is due to decreased mobility of molecular chain. Since the polymer was under thermal cycling at high temperature close to its T_g, additional cross-linking and post-curing occurred which consequently caused increase in T_g [68].

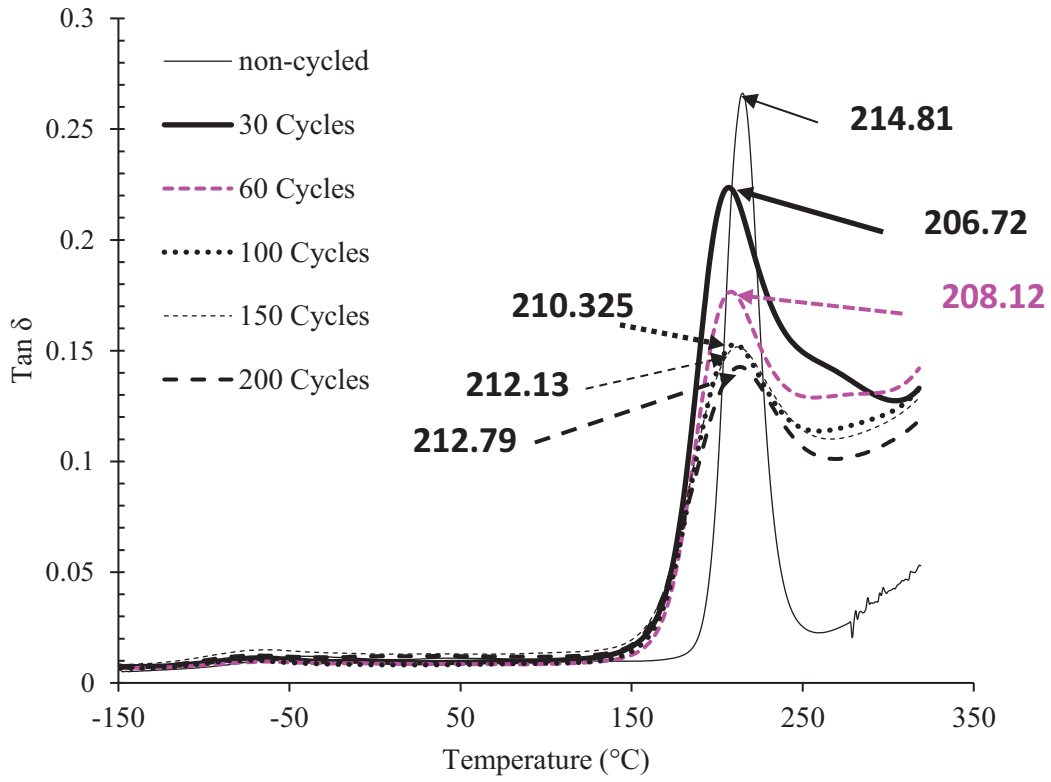

Figure 4-21 Effect of thermal cycling on tan δ of cross-ply fabric laminate in 90° direction.

Thermal cycling effect on T_g

T_g values marked in the peaks of tan δ in Figure 4-21 are listed in Figure 4-22. Unlike UD laminate, T_g drops right after 30 cycles by 3.6% from 214.8 °C to 207.1 °C and then tends to go up again to 212.79 after 200 cycles.

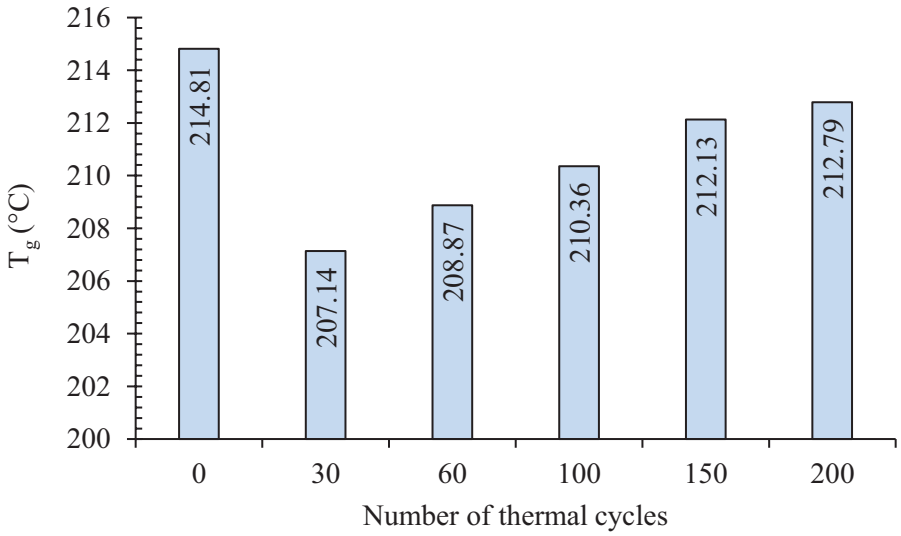

Figure 4-22 Variation of T_g of cross-ply fabric laminate vs. the number of thermal cycles.

4.2.5. Linear coefficient of thermal expansion

To measure through-the-thickness CTE, TMA tests were conducted from −70 °C to +150 °C on cross-ply fabric laminate. The effect of thermal cycling on CTE is shown in Figure 4-23. Similar to the UD laminate where CTE jumped for first 60 cycles, CTE of cross-ply fabric first increases; however, unlike the UD laminate, further thermal cycling decreases the CTE to values even lower than the CTE of unexposed sample.

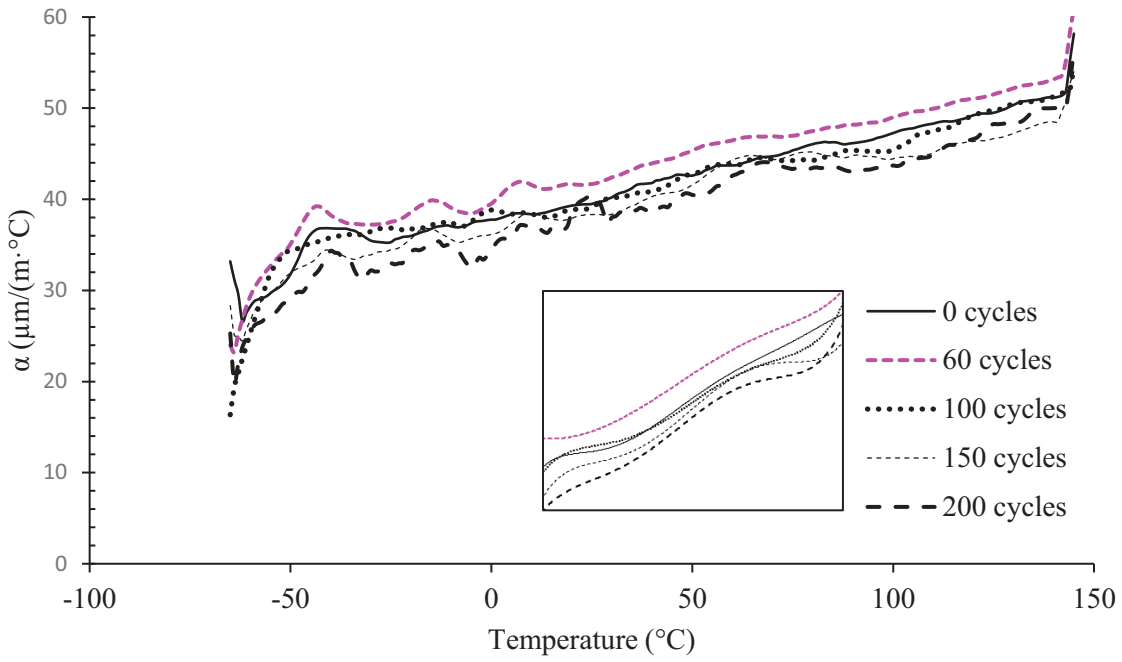

Figure 4-23 Effect of thermal cycling on through-the-thickness CTE of cross-ply fabric laminate. The inset presents polynomial trend lines fitted to CTE curves.

4.3. Sandwich panel

The effect of thermal cycling on the sandwich panel was also studied in this research. For the sandwich panel, only microscopy observation was conducted. Figure 4-25 shows the microscopic images taken from the sample cross section after 1, 2, 3, 4, 5, 10, 20, and 30 thermal cycles. As can be seen, cracks started to initiate from the first cycle. After just one cycle, horizontal cracks in the form of delamination started to grow on the core side of the sandwich panel between the adhesive and the skin. No presence of vertical cracks was observed at this stage. In this particular fabric which is woven type, when a delamination crack between the adhesive and a 90° fiber tow reached a 0° fiber tow, it jumped the 0° tow and continued to propagate horizontally beside the next 90° fiber tow. With further cycling up to 10 thermal cycles, delamination cracks continued to open and both crack length and crack width increased while new delamination were forming only on the core side of the sandwich panel. After 10 thermal cycles, vertical cracks started to form and increased in density by increasing the number of thermal cycles. The vertical crack growth stopped when it reached 0° tow; however, when the vertical crack reached 90° or 45° tows, it continued to grow and pass through them. After 30 thermal cycles,

delamination cracks propagated through the whole length of the cross section in parallel with the 90° tow. It should be mentioned that all the delaminations were observed on the core side of the panel and not on the mold (or bag) side. Besides, vertical cracks continued to grow through the thickness of skin without any significant increase in density.

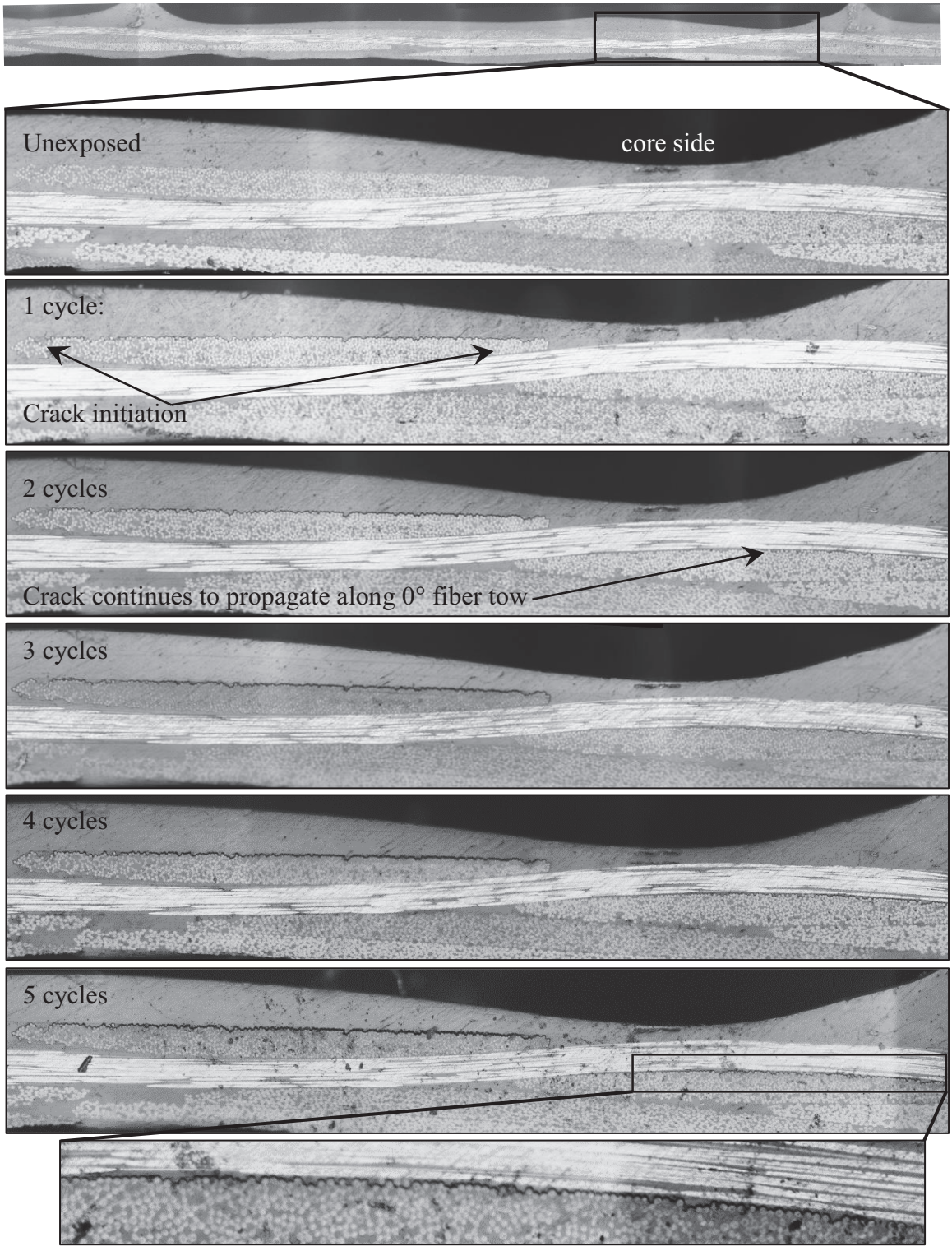

Figure 4-24 Optical microscope image of sandwich panel. Crack initiation and propagation before exposure to thermal cycling and after 1, 2, 3, 4, and 5 cycles are depicted.

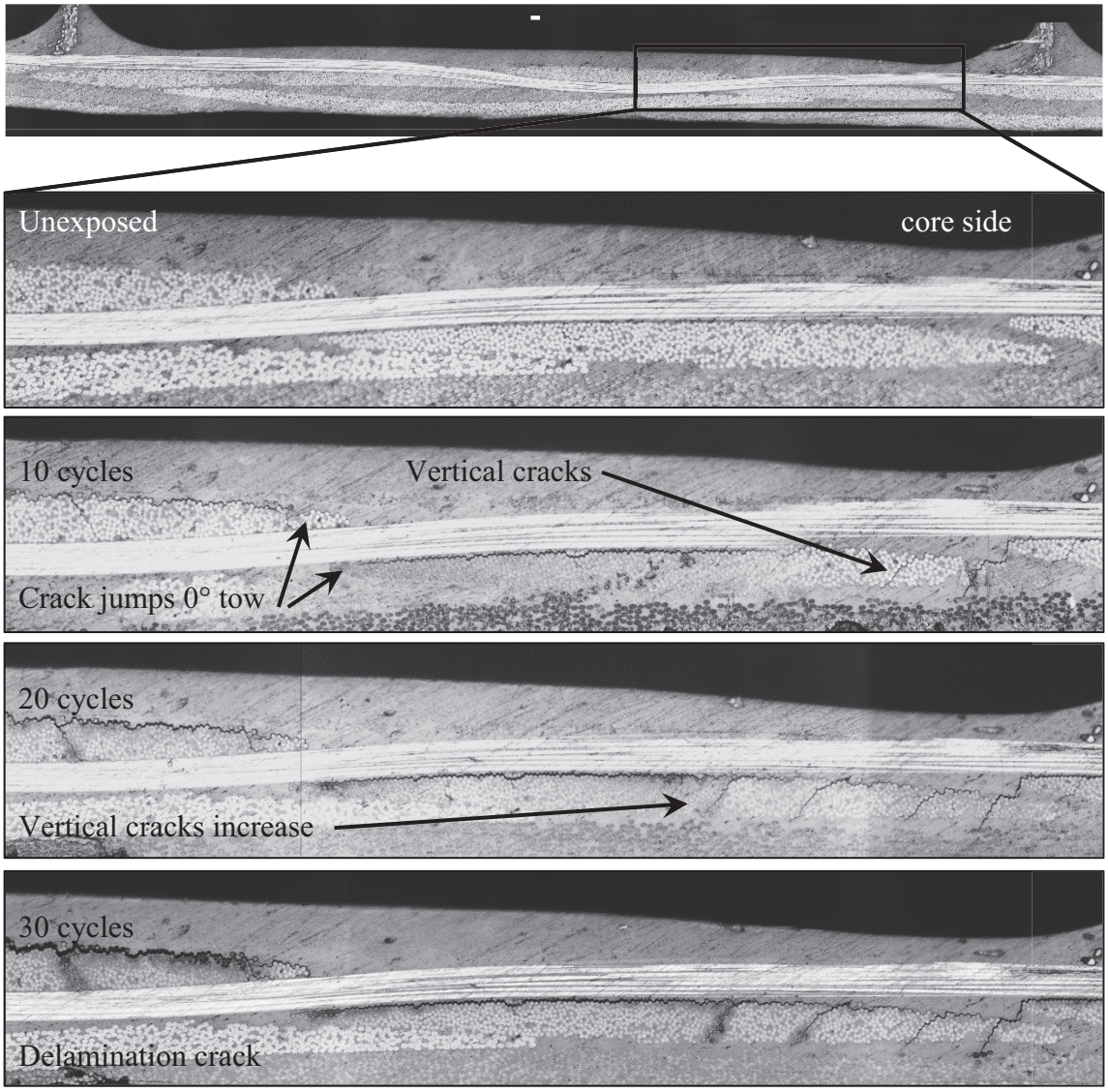

Figure 4-25 Optical microscope image of sandwich panel after exposure to 10, 20, and 30 cycles. Vertical and horizontal cracks are depicted. Delamination happens at 30 cycles.

4.4. Discussion

Here, the effort is to find the connections between the experimental results and the factors affecting them. Thermal cycling may affect the properties of carbon fiber polymer composites in two different ways: by excessive cross-linking in polymer chain due to post-curing and/or by inducing damages due to the CTE mismatch in form of matrix

cracking or fiber/matrix debonding. These two competing factors are briefly explained in the following.

During thermal cycling at high temperatures (particularly close to curing temperature), the temperature rise can induce post-curing to some extent and cause the improvement of crosslinking degrees of the resin matrix [49], which in turn may improve some physical and mechanical properties. Alternatively, during thermal cycling test, both fiber and matrix in the composite are frequently exposed to severe temperature changes from −196°C to +140 °C, and each of them behaves in a different way. By increases of temperature, the carbon fiber contracts and matrix expands due to different CTEs. As a result of thermal cycling, CTE difference (or CTE mismatch) induces cyclic thermal stresses whose maximum is at −196 °C. Thermal stresses in polymer composites could create microcracks in the polymer and also fiber/matrix debonding, which could simply grow and propagate within the structure which consequently prevents efficient load transfer and lead to damages and change the properties [7], [11], [69]- [71]. It should be emphasized that in the matter of competing effect between the cross-linking and the matrix cracking, the whole specimen should be considered and not only its surface. In this research, however, the microscopy was done only on the surface and no information on the possible internal damages, if there was any, was collected. Mostly, the chance of having cracks in the surface due to the CTE mismatch seems to be higher because the specimens was not confined and could freely and symmetrically expand/contract in all directions.

In terms of void content after curing, no void was observed in the sandwich panel specimens, while both UD and cross-ply fabric laminates had voids due to the OOA curing of the material and absence of oven pressure during the cure.

In UD specimens, no crack was observed before 350 thermal cycles (Figure 4-2); after 350 cycles, two types of horizontal cracks started to form and propagate: one in the form of delamination crack (crack between two adjacent plies) and the other within a single ply. It seems that both crack types were formed around the areas with higher void content in a such a way that the crack passed through the adjacent voids and propagated by connecting them together. Delamination cracks caused delamination between the adjacent plies and cracks within a single ply sometimes propagated and reached a delamination

crack. No vertical microcrack was observed in UD laminate. on the contrary, both cross-ply fabric laminate and sandwich panel demonstrated several microcracks in early cycles. Particularly in cross-ply fabric laminate, the vertical microcracks appeared after only one thermal cycle in the 90˚ fiber tow near the sample edge (Figure 4-14). With further cycling microcrack density in the outer layers increased and then stabilized up to 10 thermal cycles. Conversely, the microcracks in the inner layers initiated after 5 thermal cycles. Then, with the increase of number of thermal cycles up to 40 (Figure 4-15), number of inner microcracks also increased and damage continued to progress in the inner layers. No debonding between the fiber and the matrix was observed up to 40 thermal cycles for the cross-ply fabric laminate. All the cracks were vertical around the voids or edges and tended to grow through the whole thickness of the 90˚ fiber tows, as shown in Figure 4-14 and Figure 4-15.

For the sandwich panel, horizontal cracks in form of delamination started from the first cycle in the core side of the sandwich between skin and adhesive, while vertical cracks initiated after 10 cycles. Delamination (horizontal) cracks when reached a 0˚ tow passed over it and continued to grow in the next 90˚ tows while vertical cracks reaching 0˚ tow stopped. Therefore, with additional cycles, delamination crack length increased and grew along the core instead of propagating into adjacent layers. Delaminations were all observed in core side, so the presence of the adhesive in the sandwich plates influences the state of damage of the plate. Generally, the width of all vertical cracks in both sandwich panel and cross-ply fabric laminate varied across the 90° fiber tows and tapered while approaching adjacent 0° layer indicating the constraints imposed from the adjacent 0˚ tow, as observed by other researchers [37].

The interlaminar shear strength (ILSS) of UD and cross-ply fabric laminates measured by short beam shear tests was affected by thermal cycling in different ways. The ILSS of UD laminate was not actually influenced by the thermal cycles up to 200 times while ILSS of cross-ply fabric laminate was significantly affected and reduced by ~10%. These results are in agreement with the microscopy observation where vertical cracks were observed in cross-ply fabric laminate from the first cycle, while no crack (at least on the surface) was observed up to 200 thermal cycles in UD laminate. Therefore, in the case of cross-ply fabric laminate, CTE mismatch and internal damages due to induced thermal stresses

played a dominant role in competition with post-curing effect such that by increase of crack density in cross-ply fabric laminate its ILSS decreased. Conversely, cross-linking and the matrix cracking had almost equal effect on the UD laminate up to 200 thermal cycles where the ILSS test results indicated no significant change, and no further ILSS test was performed after 200 thermal cycles. It should be highlighted that the coefficient of variation (CV) in ILSS results of UD sample was of the same order as the changes in the mean value, despite some fluctuation in mean values, therefore ILSS of UD did not practically change which is in agreement with the fact that no crack was found in 200 times cycled sample. As it was shown in Figure 2-4 (d) in literature review chapter, such a trend was also reported by Gao *et al.* [47] who studied thermal cycling of UD carbon/epoxy composite. They mentioned that this behavior is mainly due to the changes in the shear strength of the epoxy which would vary with the density of the cross-linking. In the case of laminates studied in this research, DSC results showed that the cross-ply fabric laminate reached a higher degree of cure than UD laminate, therefore post-curing during thermal cycling of UD could occur at a greater extent compared with cross-ply laminate.

The results of dynamic mechanical analysis (DMA) is also in agreement with ILSS results. The storage modulus (E′) of cross-ply fabric laminate compared with UD laminate decreased significantly by the increase of the number of thermal cycles; particularly at room temperature, $E'_{cross\text{-}ply}$ decreased by ~23% after exposure to 200 thermal cycles, while E'_{UD} decreased less than 4%. On the other hand, since at room temperature tan δ is very small (tan $\delta \approx 0$), therefore the storage modulus at room temperature is almost equal to the complex modulus E^* whose value is proportional to the elastic modulus. Therefore, it is expected that the storage modules at room temperature and stiffness properties of the material, such as ILSS, are affected in almost the same way by the thermal cycling. Thus, in the case of cross-ply fabric laminate, ILSS and storage modulus were both significantly affected by the thermal cycling which increased the crack density, whereas these properties in the case of UD laminate are not influenced by the number of thermal cycling examined. These results are also in good agreement by microscopy results. The fact that E'_{UD} did not change significantly up to 350 thermal cycles (~3% decrease) indicates that the damage induced to the matrix material before

350 thermal cycles was not big enough which conforms to the microscopy observations. In the same way for cross-ply fabric laminate, the reduction of storage modulus by increase of thermal cycles is an indication of increase in the number of microcracks which is in agreement with the observations by optical microscopy where microcracks initiated from early cycles. It is worth mentioning that the changes in storage modulus measured by DMA is mainly related to changes in the polymer. The reason for this is that in three-point bending test of UD laminate in DMA, fibers are perpendicular to the bending load and thus the properties measured by DMA are more related to the structural changes in the polymer matrix [66], [72].

T_g, which is obtained from the peak of tan δ in DMA tests in the present research, can be used to determine the crosslinking degree of the resin matrix. It is known that with a higher level of crosslinking in the resin matrix, a higher temperature is needed to pass the elastic region and reach the elastomeric state [7], [11]. The trend of T_g variation with respect to the number of thermal cycles for UD (Figure 4-11) is different from that of cross-ply fabric laminate (Figure 4-22). There was a slight increase of 1.6% in T_g of UD laminates until 150 thermal cycles followed by a 7.4% decrease up to 350 cycles. Such a trend, which was already observed by other researchers [7], [11], [47], [73], is believed to be due to the increase in the degree of crosslinking of the resin caused by the temperature rising during first 150 thermal cycles and post-curing effect to some extent. It should be remembered that degree of cure for UD and cross-ply fabric laminate was ~94% and ~98%, respectively, which confirms higher possibility of post-curing for UD in comparison with cross-ply fabric laminate. As thermal cycles increase from 150, it seems that there is no further curing but probably some internal damages due to CTE mismatch initiated and increased. As a result, T_g of UD laminate gradually decreases after 150 cycles. T_g results show that the CTE mismatch effect arises after 150 thermal cycles while microscopic evaluations of cycled samples indicate the crack presence from 350 thermal cycles. It seems that the damage due to the CTE mismatch was not big enough in its initial stage to be detected or cracks were properly formed inside the composite. By the increase in the number of cycles cracks propagated and grew enough to be visible from 350 thermal cycles. Besides, the loss modulus values obtained from DMA tests also confirms this behavior; insignificant increase during the first 150 cycles, and then

continuous increase up to 350 cycles. Unlike UD laminate, T_g of cross-ply laminate had a reduction of 3.6% after 30 cycles followed by an increase of 2.7% after 30 cycles. The initial decrease could be due to the increasing level of crack density which was also observed in microscopy images, whereas the following increase was probably caused by excessive cross-linking in resins. This is also in agreement with previous results; e.g, storage modulus of the cross-ply laminate reduced due to the increase of crack density. Peak of tan δ for both UD and cross-ply laminate decreased by the increase of thermal cycles, which was more significant for cross-ply laminate. Moreover, the curve at peak of cross-ply laminate broaden to a greater extent compared with UD laminate. This indicates that stiffness increased while viscosity decreased which probably is due to decreased mobility of molecular chain. Since the polymer was under thermal cycling at high temperature close to its T_g, additional cross-linking and post-curing occurred which consequently caused increase in T_g [68].

CTE is dependent on the temperature and also affected by the thermal cycling. For both UD and cross-ply laminate, CTE through the thickness was positive and increased with increasing the temperature. It should be remembered that CTE of carbon fibers in transverse and longitudinal direction is positive and negative, respectively, and the polymer CTE is positive in all directions. Therefore, for carbon fiber reinforced composites, lamina CTE could be negative in fiber direction, but positive in transverse direction. Moreover, in the transverse direction, CTE is matrix dominant. In the case of UD laminate, CTE jumped to a higher value when exposed to 60 cycles (about 13% higher at room temperature) followed by a slight decrease compared with its initial jump by further cycling to 200 cycles. Thus, thermal cycling caused an increase in CTE through-the-thickness of the UD laminate in a wide range of temperature. This increase became more significant at higher temperatures. Since UD laminate was not fully cured, further cycling caused further cross-links in the polymer chain and CTE increased. CTE of the cross-ply fabric laminate first increased during the first 60 cycles, similar to CTE of UD laminate; however, further thermal cycling decreased its CTE even lower than the CTE of unexposed sample. The first increased could be explained by the post-curing as the fabric laminate was not fully cured. As observed by the microscopy, further cycling

increased the crack density of the matrix which resulted in loss of the matrix integrity and consequently CTE reduction which was also reported by other researchers [11], [45].

Chapter 5: Conclusions and future works

5.1. Conclusions

In this study, the effects of thermal cycling on the mechanical and thermal properties of flat laminates made of carbon/epoxy prepregs manufactured out-of-autoclave (OOA) was examined. The study was conducted on both uni-directional tape laminate (UD) and cross-play 5HS fabric laminates of same thickness, exposed to different number of thermal cycles (30 to 350 cycles) in a temperature range from −196 °C to +140 °C. A sandwich panel was studied as well in order to find out the adhesive effect on the damage as a result of thermal cycling. Several experimental testing were conducted to characterize different mechanical and thermal properties and the main affecting factors influencing these properties were identified. It was found that the variation of different properties due to the thermal cycling could be described by a competing effect between two main factors: (i) excessive cross-linking in the polymer chain and post-curing due to the temperature rise in thermal cycles; (ii) induced damages in the form of matrix cracking or fiber/matrix debonding due to the CTE mismatch.

The following points summarize the specific conclusions drawn from the results of the current work:

- The average degree of cure measured by DSC for the UD and cross-ply laminate was 94.03% and 98.00%, respectively, which indicates a better curing degree for the cross-ply laminate.
- Optical microscopy observation revealed that horizontal cracks were initiated in the UD laminate after 350 thermal cycles in the form of delamination, whereas both cross-ply fabric laminate and sandwich panel demonstrated several microcracks in early cycles. All the cracks in the cross-ply laminate were vertical around the voids or edges (no de-bonding), while horizontal cracks were observed in the sandwich panel in the form of delamination in the core side between the skin and adhesive and vertical cracks initiated after 10 cycles.
- The interlaminar shear strength (ILSS) was measured by short beam shear tests in three-point bending. Thermal cycling affected the ILSS of UD and cross-ply fabric laminates in different ways; the ILSS of UD laminate was not actually influenced by the thermal cycles up to 200 cycles and its variation was within the coefficient of variation of the results, whereas the ILSS of the cross-ply fabric laminate was reduced by ~10%. This results are in agreement with the microscopy observations and previous research work [47] as well.
- Viscoelastic properties of laminates were examined by dynamic mechanical analysis (DMA). As expected, the thermal cycling affected the storage modulus in the same way as the ILSS, *i.e.,* by the increase of thermal cycles, the storage modulus (E′) of the cross-ply fabric laminate decreased significantly compared with the UD laminate. These results are also in good agreement with the microscopy results.
- Glass transition temperature (T_g) was obtained from the peak of tan δ in DMA tests. It was found that T_g is affected by thermal cycling, however, the trend of variations for UD and cross-ply laminate is different. In the case of UD laminate, T_g increased slightly after 150 cycles due to the dominant effect of cross-linking indicating less curing degree, and then decreased to a greater extent due to the internal damages [7], [11], [47], [73]. The loss modulus variation also confirms such a behavior. Unlike UD laminate, T_g of the cross-ply laminate reduced after

30 cycles due to the dominant effect of crack density and then increased probably as a result of excessive cross-linking in the resin.

- Coefficient of thermal expansion (CTE) through the thickness of the laminate was measured by TMA. It was found that CTE through the thickness is mainly matrix dominant, has a positive value, and increases with increasing the temperature. Moreover, CTE was affected by the thermal cycling: CTE of the UD laminate jumped to a higher value when exposed to 60 cycles owing to the further cross-links in the polymer chain and post-curing; whereas CTE of the cross-ply fabric laminate first increased after exposure to 60 cycles due to the post-curing (same as UD), and then decreased as a result of increased crack density in the matrix and loss of its integrity [11], [45].

This study may contribute to a better understanding of how two aforementioned competing factors due to the thermal cycling may affect mechanical and thermal properties of composites, thus leading to a better design in real applications

5.2. Propositions for future works

Thermal cycling effect on long term performance of carbon polymer composites was investigated in this research but there are still areas to work on in the future.

Thermal properties of the UD laminates studied in this project were affected by thermal cycling but optical microscopy of the laminate surface did not reveal any damage on the sample surface until 350 thermal cycles while DMA results indicated presence of damage in the laminate after 150 cycles. A more precise damage detection method should be developed to identify the damage inside the UD laminates as soon as they begin to form. Moisture test could be one of the alternative methods for damage detection. In this method, the composite sample should be exposed to aqueous or humid environment and then the weight changes should be measured. Increasing of water uptake in composites could be a sign of presence of microcracks inside the specimen. A maximum value for water absorption can be an indication of saturation in crack density caused by thermal cycles.

In this thesis, the cross-linking degree due to thermal cycling was evaluated by the variations in the material properties (T_g, CTE, ILSS), which is an indirect method. Even though the variations of all these studied properties agreed with the justified degree of cross-linking, it would be more accurate if one can use a direct way of measuring cross-linking density, such as rheology testing, as an indication of post cure.

Generally, in order to be better simulate the effect of thermal cycling in space, a higher number of cycles seems to be more realistic. Even though thermal and mechanical properties examined here were influenced by a limited number of thermal cycles in this research, higher number of cycles such as 1000 cycles or more is a better representative of real condition and the affected properties might have a more apparent trend or behavior with respect to number of thermal cycles. However, an automatic thermal cycling setup capable of performing higher number of cycles in vacuum on larger samples is required to be designed to be able to examine other properties such as tensile, compression, and flexural tests. A setup with the capability of heating or cooling at a controlled rate is essential to determine the effect of cooling/heating rate on damage initiation.

To the best knowledge of author, there is not enough research work on the thermal cycling of sandwich panels. Study of crack formation and propagation in the sandwich panel was initiated in this research. Further investigations on the effect of thermal cycling on the mechanical and thermal properties of sandwich panel is necessary. The sandwich panel studied here had a Kevlar core; examining sandwich panels with other cores such as Aluminum is also of the interest of space industry and could be another area of the research.

Different stacking sequences should be examined to find the layup that is more resistant to the damages induced by thermal cycles. Even though most of the research works so far has been done on the thermal cycling of UD laminates with different layups, there are not enough work on composites made of woven fabrics with different layups.

References

[1] P. K. Mallick, *Fiber-Reinforced Composites: Materials, Manufacturing and Design.* CRC Press, 2008.

[2] S. P. Rawal and J. W. Goodman. "Composites for spacecraft," in *Comprehesive Composite Materials*Anonymous 2000.

[3] S. Mazumdar, *Composites Manufacturing: Materials, Product, and Process Engineering.* CRC press, 2001.

[4] *The Space Environment*. Available: https://www.faa.gov/other_visit/aviation_industry/designees_delegations/designee_types/ame/media/Section%20III.4.1.2%20The%20Space%20Environment.pdf.

[5] J. Han and C. Kim, "Low earth orbit space environment simulation and its effects on graphite/epoxy composites," *Composite Structures,* vol. 72, pp. 218-226, 2006.

[6] P. George and H. Dursch, "Low earth orbit effects on organic composites flown on the long duration exposure facility," *J. Adv. Mater.,* vol. 25, pp. 10-19, 1994.

[7] H. Jianping *et al*, "Effects of thermal cycling on mechanical and physical properties of high performance carbon-epoxy composites applied to satellite antenna," *Xi'an Aerospace Composite Materials Institute, China,* 2014.

[8] J. Li and S. Yan, "Thermally induced vibration of composite solar array with honeycomb panels in low earth orbit," *Appl. Therm. Eng.,* vol. 71, pp. 419-432, 10/5, 2014.

[9] S. Tompkins and S. L. Williams, "Effects of thermal cycling on mechanical properties of graphite polyimide," *J. Spacecraft Rockets,* vol. 21, pp. 274-280, 1984.

[10] S. Rouquie *et al*, "Thermal cycling of carbon/epoxy laminates in neutral and oxidative environments," *Composites Sci. Technol.,* vol. 65, pp. 403-409, 2005.

[11] Q. Yu *et al*, "Effects of vacuum thermal cycling on mechanical and physical properties of high performance carbon/bismaleimide composite," *Mater. Chem. Phys.,* vol. 130, pp. 1046-1053, 2011.

[12] I. Tsukrov, B. Drach and T. Gross, "Effective stiffness and thermal expansion coefficients of unidirectional composites with fibers surrounded by cylindrically orthotropic matrix layers," *Int. J. Eng. Sci.,* vol. 58, pp. 129-143, 2012.

[13] J. Sanborn and D. Morel, "Effects of thermal cycling on the mechanical and physical properties of a space qualified epoxy adhesive," *J Reinf Plast Compos,* vol. 7, pp. 155-164, 1988.

[14] C. Henaff-Gardin and M. Lafarie-Frenot, "Specificity of matrix cracking development in CFRP laminates under mechanical or thermal loadings," *Int. J. Fatigue,* vol. 24, pp. 171-177, 2002.

[15] T. Shimokawa *et al*, "Effect of thermal cycling on microcracking and strength degradation of high-temperature polymer composite materials for use in next-generation SST structures," *J. Composite Mater.,* vol. 36, pp. 885-895, 2002.

[16] V. T. Bechel, J. D. Camping and R. Y. Kim, "Cryogenic/elevated temperature cycling induced leakage paths in PMCs," *Composites Part B: Engineering,* vol. 36, pp. 171-182, 3, 2005.

[17] M. W. Hyer, *Stress Analysis of Fiber-Reinforced Composite Materials.* DEStech Publications, Inc, 2009.

[18] C. R. Nair, D. Mathew and K. Ninan, "Cyanate ester resins, recent developments," in *New Polymerization Techniques and Synthetic Methodologies*Anonymous Springer, 2001, pp. 1-99.

[19] *Guide to Composites*. Available: http://www.gurit.com/files/documents/guide-to-compositesv5webpdf.pdf.

[20] *Working with epoxy resin*. (05/29/2015). Available: https://davidneat.wordpress.com/tag/price-of-epoxy-resin/

[21] G. Rabilloud, *High-Performance Polymers.* Paris: Editions OPHRYS, 1999.

[22] A. Shanker, R. W. Sullivan and D. A. Drake, "Elastic properties of CYCOM 5320-1/T650 at elevated temperatures using response surface methodology," in *Composite, Hybrid, and Multifunctional Materials, Volume 4*Anonymous Springer, 2015, pp. 29-37.

[23] K. Jackson and M. Crabtree, "Autoclave quality composites tooling for composite from vacuum bag only processing," in *47 Th International SAMPE Symposium and Exhibition 2002,* 2002, pp. 800-807.

[24] L. Repecka and J. Boyd, "Vacuum-bag-only-curable prepregs that produce void-free parts," in *47 Th International SAMPE Symposium and Exhibition 2002,* 2002, pp. 1862-1874.

[25] F. C. Campbell, "Curing," in *Manufacturing Technology for Aerospace Structural Materials,* Elsevier Ltd, 2006.

[26] B. W. Grimsley *et al*, "Elevated temperature, notched compression performance of out of autoclave processed composites," *NASA Langley Research Center, Hampton, VA, United States,* 2013.

[27] J. K. Sutter *et al*, "Comparison of autoclave and out-of-autoclave composites," *NASA Research Center,* 2010.

[28] P. L. Chiou and P. K. Oldroyd, "Out of autoclave material and process for sandwich structures," in *52nd International SAMPE Symposium,* Long Beach, CA, United States, 2008, .

[29] J. Cauberghs, "Out-of-Autoclave Manufacturing of Aerospace Representative Parts.", 2012.
Available:
http://digitool.library.mcgill.ca/webclient/StreamGate?folder_id=0&dvs=1485749277122~22

[30] K. S. Madhok, Thesis (Masters), Concordia University, 2013. Available: http://spectrum.library.concordia.ca/978552/

[31] V. T. Bechel, M. Negilski and J. James, "Limiting the permeability of composites for cryogenic applications," *Composites Sci. Technol.,* vol. 66, pp. 2284-2295, 2006.

[32] V. T. Bechel and R. Y. Kim, "Damage trends in cryogenically cycled carbon/polymer composites," *Composites Sci. Technol.,* vol. 64, pp. 1773-1784, 2004.

[33] V. T. Bechel *et al*, "Effect of stacking sequence on micro-cracking in a cryogenically cycled carbon/bismaleimide composite," *Composites Part A: Applied Science and Manufacturing,* vol. 34, pp. 663-672, 2003.

[34] J. F. Timmerman *et al*, "Matrix and fiber influences on the cryogenic microcracking of carbon fiber/epoxy composites," *Composites Part A: Applied Science and Manufacturing,* vol. 33, pp. 323-329, 2002.

[35] M. Lafarie-Frenot, "Damage mechanisms induced by cyclic ply-stresses in carbon–epoxy laminates: Environmental effects," *Int. J. Fatigue,* vol. 28, pp. 1202-1216, 2006.

[36] C. T. Herakovich and M. Hyer, "Damage-induced property changes in composites subjected to cyclic thermal loading," *Eng. Fract. Mech.,* vol. 25, pp. 779-791, 1986.

[37] D. S. Adams, D. E. Bowles and C. T. Herakovich, "Thermally induced transverse cracking in graphite-epoxy cross-ply laminates," *J Reinf Plast Compos,* vol. 5, pp. 152-169, 1986.

[38] C. Henaff-Gardin, M. Lafarie-Frenot and D. Gamby, "Doubly periodic matrix cracking in composite laminates Part 1: general in-plane loading," *Composite Structures,* vol. 36, pp. 113-130, 1996.

[39] D. Isaac M. and O. Ishai, Engineering Mechanics of Composite Materials. NY: Oxford univ. press, 1994.

[40] S. S. Kessler, T. Matuszeski and H. McManus, "Cryocycling and Mechanical Testing of CFRP for X-33 Liquid H2 Fuel Tank Structure," *Proceedings of the American Society for Composites (ASC),* 2001.

[41] J. Ajaja and F. Barthelat, "Damage accumulation in a carbon fiber fabric reinforced cyanate ester composite subjected to mechanical loading and thermal cycling," *Composites Part B: Engineering,* vol. 90, pp. 523-529, 4/1, 2016.

[42] P. Dutta *et al*, "Response of advanced composite space materials to thermal cycling," *Engineering, construction, and operations in space; Proceedings of the Space '88 Conference, UNITED STATES;* 29-31 Aug. 1988

[43] P. K. Dutta, "Structural fiber composite materials for cold regions," *J. Cold Regions Eng.,* vol. 2, pp. 124-134, 1988.

[44] S. Y. Park *et al*, "Effect of vacuum thermal cyclic exposures on unidirectional carbon fiber/epoxy composites for low earth orbit space applications," *Composites Part B: Engineering,* vol. 43, pp. 726-738, 3, 2012.

[45] K. Shin *et al*, "Prediction of failure thermal cycles in graphite/epoxy composite materials under simulated low earth orbit environments," *Composites Part B: Engineering,* vol. 31, pp. 223-235, 4/1, 2000.

[46] G. A. Owens and S. E. Schofield. Thermal cycling and mechanical property assessment of carbon fibre fabric reinforced PMR-15 polyimide laminates. *Composites Sci. Technol. 33(3),* pp. 177-190. 1988. DOI: http://dx.doi.org/10.1016/0266-3538 (88)90059-0.

[47] Y. Gao *et al*, "Effect of vacuum thermo-cycling on physical properties of unidirectional M40J/AG-80 composites," *Composites Part B: Engineering,* vol. 36, pp. 351-358, 6, 2005.

[48] R. W. Grenoble, "Mechanical Properties and Durability of a Composite Material at Cryogenic Temperatures." *Mechanical properties and durability of a composite material at cryogenic temperatures,* 2006.

[49] S. S. Tompkins, "Effects of thermal cycling on composite materials for space structures," in *NASA (SDIO) Space Environmental Effects on Materials Workshop, Part 2; P 447-470,* United States, 1989, pp. 447-470.

[50] S. S. Tompkins, J. Y. Shen and A. J. Lavoie, "Thermal cycling of thin and thick ply composites," *Proceedings of Space '94 Sponsored by the Aerospace Division/ASCE Albuquerque, New Mexico,* 1994.

[51] J. F. Timmerman *et al*, "Matrix and fiber influences on the cryogenic microcracking of carbon fiber/epoxy composites," *Compos Part A: Appl Sci Manuf,* vol. 33, pp. 323-329, 2002.

[52] S. Wang *et al*, "Influence of liquid nitrogen steeping on mechanical properties of a unidirectional carbon fiber reinforced bismaleimide composite," *Polym. Polym. Compos.,* vol. 22, pp. 129, 2014.

[53] *cycom® 5320-1 epoxy resin system technical data sheet*. (October 2015). Available: https://www.cytec.com/sites/default/files/datasheets/CYCOM%205320-1%20Rev%20CR5.pdf

[54] R. Parambath Mohan, "Investigation of Intra/Ply Shear Behavior of Out-of-Autoclave Carbon/Epoxy Prepreg.", Thesis (Masters), 2015. Available: http://spectrum.library.concordia.ca/979766/

[55] S. V. Hoa, *Principles of the Manufacturing of Composites Materials.* DEStech Publications, 2009.

[56] "Cycom 5320-1 Epoxy Resin System- Technical Data Sheet," unpublished.

[57] *Introducing the DSC Q series*. Available: http://www.nt.ntnu.no/users/deng/other%20stuff/DSC_manuals/QDSC/Introducing_the_DSC_QSeries.htm

[58] *Q200 Differential Scanning Calorimeter (DSC)*. Available: https://berc.ku.edu/thermal-mechanical-analysis

[59] *Q400 Thermomechanical Analyzer*. Available: http://www.tainstruments.com/pdf/TMA.pdf

[60] *TMA Q400 brochure*. Available: http://www.tainstruments.com/wp-content/uploads/TMA.pdf

[61] *Q800 Dynamic Mechanical Analyzer*. Available: http://www.tainstruments.com/pdf/brochure/dma.pdf

[62] A. Saha *et al*, "Study of jute fiber reinforced polyester composites by dynamic mechanical analysis," *J Appl Polym Sci,* vol. 71, pp. 1505-1513, 1999.

[63] https://en.wikipedia.org/wiki/Dynamic_mechanical_analysis#cite_note-Nair-4 ,(2016/09/11).

[64] *DMA Q800 brochure*. Available: http://www.tainstruments.com/wp-content/uploads/dma.pdf

[65] F. H. Chowdhury, M. V. Hosur and S. Jeelani, "Studies on the flexural and thermomechanical properties of woven carbon/nanoclay-epoxy laminates," *Materials Science and Engineering: A,* vol. 421, pp. 298-306, 4/15, 2006.

[66] E. J. Bosze *et al*, "High-temperature strength and storage modulus in unidirectional hybrid composites," *Composites Sci. Technol.,* vol. 66, pp. 1963-1969, 10, 2006.

[67] D. T. Wrublewski, "Mechanical evaluation methods for polymer and composite systems," 2011.

[68] W. K. Goertzen and M. R. Kessler, "Dynamic mechanical analysis of carbon/epoxy composites for structural pipeline repair," *Composites Part B: Engineering,* vol. 38, pp. 1-9, 1, 2007.

[69] P. P. Parlevliet, H. E. Bersee and A. Beukers, "Residual stresses in thermoplastic composites—A study of the literature—Part I: Formation of residual stresses," *Composites Part A: Applied Science and Manufacturing,* vol. 37, pp. 1847-1857, 2006.

[70] M. E. Adams, G. A. Campbell and A. Cohen, "Thermal stress induced damage in a thermoplastic matrix material for advanced composites," *Polymer Engineering & Science,* vol. 31, pp. 1337-1343, 1991.

[71] J. F. Timmerman and J. C. Seferis, "Predictive modeling of microcracking in carbon-fiber/epoxy composites at cryogenic temperatures," *J Appl Polym Sci,* vol. 91, pp. 1104-1110, 2004.

[72] M. Akay. Aspects of dynamic mechanical analysis in polymeric composites. *Composites Sci. Technol. 47(4),* pp. 419-423. 1993. DOI: http://dx.doi.org/10.1016/0266-3538 (93)90010-E.

[73] E. G. Wolff, *Microcracking in Graphite-Epoxy Composites,* 1980.